Title
Adaptive Vehicle Traction Control

Permalink
https://escholarship.org/uc/item/8g5701zj

Authors
Lee, Hyeongcheol
Tomizuka, Masayoshi

Publication Date
1995

Adaptive Traction Control

Hyeongcheol Lee
Masayoshi Tomizuka

University of California, Berkeley
Department of Mechanical Engineering

The contents of this report reflect the views of the authors who are
responsible for the facts and the accuracy of the data presented
herein. The contents do not necessarily reflect the official views or
policies of the State of California. This report does not constitute a
standard, specification, or regulation.

Adaptive Traction Control

Hyeongcheol Lee
Masayoshi Tomizuka

California Partners for Advanced Transit and Highways (PATH)
Department of Mechanical Engineering
University of California, Berkeley

September 1995

Abstract

This report presents two different control algorithms for adaptive vehicle traction control, which includes (1) wheel slip control, (2) optimal time control, (3) anti-spin acceleration and anti-skid control, and (4) longitudinal platoon control. The two control algorithms are respectively based on adaptive fuzzy logic control and sliding mode control with on-line road condition estimation. The motivation for investigating adaptive techniques arises from the unknown time-varying nature of the tire/road surface condition which governs vehicle traction. Simulations of the two control methods are conducted using a complex nonlinear vehicle model as well as a simple linear vehicle model. The controllers both result in improved performance, regardless of vehicle operating conditions, compared with standard fuzzy logic control and standard sliding mode control which do not have adaptive algorithms.

Keywords: Traction Control, Anti-lock Braking System, Adaptive Fuzzy Control, Sliding Mode Control.

Executive Summary

This report summarizes the final year research results of the PATH project (MOU 35) : Passive and Active Traction Control. Previous research on this topic has been performed by some conventional control approaches, such as nonlinear control methods based on sliding mode control, or direct fuzzy/knowledge based approaches. In most previous research, road condition change is not considered; or, even if it is considered, the controller has high gain characteristics for dealing with the unknown time-varying interaction between the tire and road surface.

This report is concerned with the combined use of adaptive and robust control techniques for achieving robust and smooth traction control. In particular, vehicle traction control using adaptive fuzzy logic control and adaptive sliding mode control is studied. These two control methods have adaptive algorithms to deal with the unknown time-varying tire/road surface condition in different ways. For the former, the fuzzy rule base (which includes information of tire/road surface condition) will be adjusted; and for the latter, a parameter (which represents tire/road surface condition in an assumed mathematical tire model) will be estimated.

The standard fuzzy logic control method and sliding mode control method are also described in order to compare their performance with that of the proposed controllers. Simulations are conducted using a simple vehicle model to illustrate the basic ideas lying behind these suggested adaptive control schemes. Simulations are also conducted using a complex vehicle model which describes the dynamic behavior of the vehicle as realistically as possible.

The simulation results show that the proposed controllers including adaptive algorithms can be quickly adjusted when driving conditions (e.g. road condition) are changed. By this property, the proposed controllers give more stable and robust performance on vehicle traction control than conventional control algorithms.

Tables of Contents

List of Figures and Tables

1. Introduction

Vehicle traction control is control of tire traction forces both in the longitudinal and lateral directions to obtain desired vehicle motion. The tire traction forces come from the tire/road interaction and they are decomposed in two components: one in the longitudinal direction and the other in the lateral direction. The tire traction force in the lateral direction depends on the tire slip angle and can be controlled by the steering angle (Peng and Tomizuka 1990). The traction force in the longitudinal direction, which will be considered in this report, depends on the adhesion coefficient between the tire and the road surface, which in turn depends on the wheel slip as well as the tire/road surface condition. The wheel slip is a nonlinear function of the wheel velocity and the vehicle velocity. Due to the dependency of the longitudinal traction force on the wheel slip, vehicle traction control can be achieved by wheel slip control.

Controlling the longitudinal traction can achieve various control objectives, such as

(i)   regulating the wheel slip at any desired value in order to produce a desired amount of longitudinal traction force (slip control),
(ii) maintaining the fastest stable acceleration and deceleration (minimum time control),
(iii) obtaining anti-spin acceleration and anti-skid deceleration, and
(iv) controlling vehicles longitudinally in a platoon following the vehicles in front (longitudinal platoon control).

In general there are two major difficulties involved in the design of a practical traction control algorithm:
(i) the system dynamics is highly nonlinear with time-varying parameters and uncertainties
(ii) the tire/road surface condition, on which the performance strongly depends, is time varying and not precisely known during driving.
Because of these adverse features of the system, even though several automobile companies have developed and installed a version of traction control, i.e. Anti-lock Braking Systems (ABS), their design is often experimental rather than analytical, and the tuning and calibration of ABS's rely essentially on trial error (Leiber and Czinczel 1983, Leiber et al. 1982, and Yoneda et al. 1983).

Recently, some analytical approaches to ABS controller design have been achieved. Conventional control approaches using nonlinear control methods based on sliding mode control (Tan 1988, Tan and Tomizuka 1989, Tan and Tomizuka 1990, Fling and Fenton 1981) and direct fuzzy/knowledge based approaches (Yoneda et al. 1983, Tabo et al. 1985, Gunter and Ouwerkerk 1972, and Layne et al. 1992) have been successfully implemented. Analytical approach to the all four traction control objectives has been studied by Kachroo and

Tomizuka (Kachroo and Tomizuka 1994, Kachroo 1993) using sliding mode control. In most previous research, road condition change is not considered; or, even if it is considered (e.g. Kachroo's), the controller has high gain characteristics for dealing with the unknown time-varying interaction between the tire and road surface. The results look successful, but chattering due to high gain control still remain as a problem.

This report is concerned with the combined use of adaptive and robust control techniques for achieving robust and smooth traction control. In particular, vehicle traction control for all control objectives using adaptive fuzzy logic control and sliding mode control with on-line road condition estimation is studied. These two control methods have adaptive algorithms to deal with the unknown time-varying tire/road surface condition in different ways. For the former, the fuzzy rule base (which includes information of tire/road surface condition) will be adjusted; and for the latter, a parameter (which represents tire/road surface condition in an assumed mathematical tire mode) will be estimated.

The standard fuzzy logic control method and sliding mode control method are also described in order to compare their performance with that of the proposed controllers. Simulations are conducted using a simple vehicle model to illustrate the basic ideas lying behind these suggested adaptive control schemes. Simulations are also conducted using a complex vehicle model which describes the dynamic behavior of the vehicle as realistically as possible.

2. Simple vehicle model

A simple vehicle model appropriate for both vehicle acceleration and deceleration is described in this section (figure 2.1). This model will be used for analysis and controller design as well as simulation. The simple vehicle model is obtained by assuming that

(i) the dynamics of the left and right side of the vehicle are identical (bicycle model),
(ii) vehicle mass is equally distributed among each wheel, and
(iii) the engine and suspension dynamics are ignored.

Therefore, this model contains front one-wheel rotational dynamics and linear vehicle dynamics, as well as the interaction between them. Rotational dynamics of the rear wheel is not considered since it is trivial during acceleration and identical to that of the front wheel during deceleration (for the front wheel driven model). The model identifies wheel angular velocity and vehicle velocity as state variables and wheel torque exerted from the engine and the brake as the input variable.
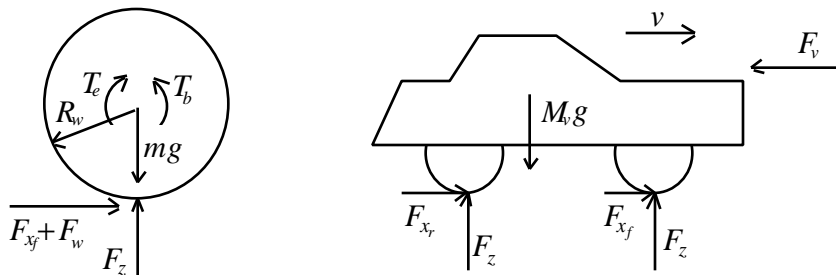
M_v: Vehicle mass $\qquad\qquad$ m: Vehicle mass exerted at the front wheel

$T_{net} = T_e - T_b$: Net torque $\qquad\qquad$ T_e: Shaft torque from the engine

T_b: Brake torque $\qquad\qquad$ F_z: Normal force

F_{xf}, F_{xr}: Traction force of the front and rear wheel

F_v: Aerodynamic friction force $\qquad$ F_w: Wheel viscose friction

Figure 2.1 Wheel model and car model

2.1 system dynamics

The dynamic equations for the angular motion of the front wheel and the longitudinal motion of the vehicle are

$$J_w \dot{\omega}_w = T_{net} - R_w \left(F_{xf} + F_w \right) \tag{2.1}$$

$$M_v \dot{v}_v = 2\left(F_{xf} + F_{xr} \right) - F_v = n_w F_{xf} - F_v \tag{2.2}$$

where ω_w is the front wheel angular velocity, v_v is the vehicle longitudinal velocity, J_w is the moment of inertia of the front wheel, and n_w is the number of driving wheels (=2) or braking wheels (=4).

When a net torque (T_{net}) is applied to a pneumatic tire, traction force will be developed at the tire-ground contact patch. At the same time, the tire tread in front of and within the contact patch is subject to compression or tension depending on whether the vehicle is in acceleration or deceleration. Consequently, the distance the tire travels when it is subject to a driving torque (braking torque) will be less (greater) than when it is free rolling. This phenomenon is usually referred to as the deformation slip or wheel slip ,λ (Wong 1978). The wheel slip of a driving wheel during acceleration and deceleration is defined as

$$\lambda = \left(R_w \omega_w - v_v \right) / R_w \omega_w \qquad \text{when } R_w \omega_w > v_v \text{ (Acceleration)}$$

$$\lambda = \left(R_w \omega_w - v_v \right) / v_v \qquad \text{when } R_w \omega_w < v_v \text{ (Deceleration)} \tag{2.3}$$

The front tire traction force is given by

$$F_{xf} = \mu(\lambda) F_z \tag{2.4}$$

where the adhesion coefficient, $\mu(\lambda)$, depends on the road condition as well as the value of the wheel slip. For various road conditions, the $\mu - \lambda$ curves have different peak values and slopes, as shown in figure 2.2.
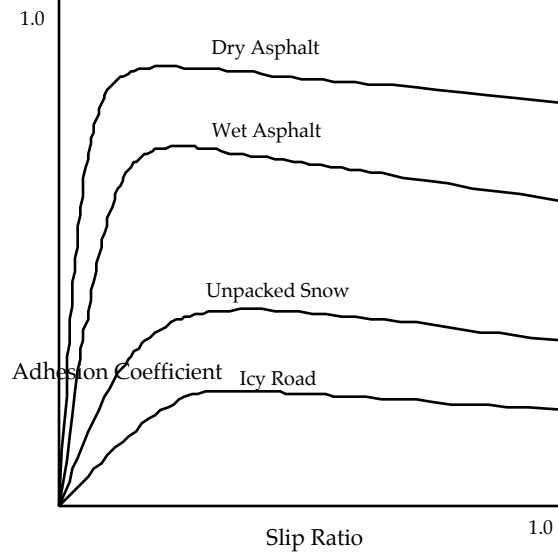
Figure 2.2 $\mu - \lambda$ curves for different road conditions

The dynamic equations of the whole system can be written in state variable form by defining convenient state variables. Defining the state variables as

$$x_1 = \frac{v_v}{R_w}, \quad x_2 = \omega_w \tag{2.5}$$

we can rewrite equations (2.1) and (2.2) as

$$\dot{x}_1 = -f_1(x_1) + b_1 \mu(\lambda) \tag{2.6}$$
$$\dot{x}_2 = -f_2(x_2) - b_2 \mu(\lambda) + b_3 T \tag{2.7}$$

where

$$\lambda = (x_2 - x_1)/x_2 \quad \text{(for } x_2 > x_1 \text{, acceleration)},$$
$$\lambda = (x_2 - x_1)/x_1 \quad \text{(for } x_2 < x_1 \text{, deceleration)},$$
$$f_1(x_1) = F_v / (M_v R_w), \qquad f_2(x_2) = F_w R_w / J_w,$$
$$b_1 = n_w F_z / (M_v R_w), \qquad b_2 = F_z R_w / J_w, \qquad b_3 = 1/J_w.$$

The control input is the applied torque at the wheels, which is equal to the difference between the shaft torque from the engine and the braking torque.

2. 2 Wheel slip dynamic equation

Wheel slip is chosen as the controlled variable for the traction control algorithm because of its strong influence on the traction force between the tire and the road. By controlling the wheel slip, we can control the traction force in order to obtain a desired output of the system. In order to control the wheel slip, it is convenient to have dynamic equations in terms of the wheel slip.

By differentiating the wheel slip ($\lambda = (x_2 - x_1)/x_2$) with respect to time, we obtain the wheel slip dynamic equation during acceleration.

$$\dot{\lambda} = \frac{\partial \lambda}{\partial x_1}\frac{\partial x_1}{\partial t} + \frac{\partial \lambda}{\partial x_2}\frac{\partial x_2}{\partial t}$$

$$= \frac{1}{x_2}\left[f_1 - (1-\lambda)f_2 - \left\{(1-\lambda)b_2 + b_1\right\}\mu + (1-\lambda)b_3 T \right] \tag{2.8}$$

Equation (2.8) is highly nonlinear and involves uncertainties in its parameters. Using the same method as that of the acceleration case, we obtain the wheel slip dynamic equation during deceleration ($\lambda = (x_2 - x_1)/x_1$).

$$\dot{\lambda} = \frac{1}{x_1}\left[(1+\lambda)f_1 - f_2 - \left\{b_2 + (1+\lambda)b_1\right\}\mu + b_3 T\right] \tag{2.9}$$

3. Design and application of controllers (for the simple vehicle model)

The system dynamics are highly nonlinear and time varying because of the dependency of the wheel slip on the road conditions. This motivates the use of sliding mode control as well as fuzzy logic control. In this section, we present the design of these controllers and comparison of the two controllers based on simulations.

3.1 Problem formulation

System equation :

The equations derived in the previous chapter, equations (2.6), (2.7), (2.9), and (2.11) can be expressed as

$$\dot{x}_1 = -f_1(x_1) + b_1 \mu(x_3) \tag{3.1}$$
$$\dot{x}_2 = -f_2(x_2) - b_2 \mu(x_3) + b_3 T \tag{3.2}$$
$$\dot{x}_3 = f_3(x_1, x_2) - f_4(x_3)\mu(x_3) + f_5(x_3)T \tag{3.3}$$

where x_3 is the wheel slip.

Control objectives (Slip control) :

Find a control law for the input torque, T, such that the tracking error, $x_3(t) - x_{3d}(t)$, goes to zero, while all the state variables remain bounded.

Important physical properties :

We should note the following two points related to the system equation.

(i) The system equations are nonlinear and involves uncertainties. Nonlinearities include the defining equation of the wheel slip, the $\mu - \lambda$ relationship, multiple terms of states and the wheel slip, and the functions $f_1(x_1)$, $f_2(x_2)$, and $f_3(x_1, x_2)$.

(ii) $f_1(x_1)$ and $\mu(x_3)$, which express the wind drag and the friction coefficient between the tire and road surface, respectively, are unknown and time varying functions during driving. Since $f_1(x_1)$ does not

significantly affect system performance, we will focus on how to deal with the unknown function, $\mu(x_3)$, in this report.

3.2 Controller description

Because of the unknown functions in the state equation, we will consider the following two control methods which include adaptive algorithms.

(i) Sliding mode control with on-line road condition estimation
(ii) Adaptive fuzzy logic control

3.2.1 Sliding mode control with on-line road condition estimation

3.2.1.1 Sliding mode controller

Consider an nth-order nonlinear system of the canonical form:

$$x^{(n)} = f(\mathbf{x}) + bu, \qquad y = x \tag{3.4}$$

where the scalar x is the output of interest, $\mathbf{x} = \left[x, \dot{x}, \cdots, x^{(n-1)} \right]^T$ is the state vector, $f(\mathbf{x})$ is a nonlinear function of the state which includes uncertainties, the control gain b is known and includes negligible uncertainties, and u is the control input. This equation has a general form, but, in fact, it is the same as equation (3.3) when $n = 1$. The control objective is to make the output track a desired time-varying trajectory $\mathbf{x}_d = \left[x_d, \dot{x}_d, \cdots, x_d^{(n-1)} \right]^T$. Let

$$\mathbf{e} = \mathbf{x} - \mathbf{x}_d = \left[e, \dot{e}, \cdots, e^{(n-1)} \right]^T \tag{3.5}$$

be the tracking error vector. Furthermore, let us define a time-varying surface $S(t)$ in the state-space by the scalar equation $s(\mathbf{x};t) = 0$, where

$$s(\mathbf{x};t) = \left(\frac{d}{dt} + \lambda \right)^{(n-1)} e$$
$$= \Lambda^T \mathbf{e} \tag{3.6}$$

and $\Lambda^T = \left(\lambda^{(n-1)}, (n-1)\lambda^{(n-2)}, \cdots, \lambda \right)$, λ is a strictly positive constant. Then, the problem of tracking $\mathbf{x} \equiv \mathbf{x}_d$ is equivalent to that of remaining on the surface $S(t)$ for all $t > 0$. Thus, the problem of tracking the n-dimensional vector $\mathbf{x}_d$ can be reduced to that of keeping the scalar quantity s at zero. This means that we have in effect replaced an nth-order tracking problem by a first-order stabilization problem. This simplified first-order problem of keeping the scalar s at zero can now be achieved by choosing the control law u such that outside of $S(t)$

$$\frac{1}{2} \frac{d}{dt} s^2 \leq -\eta |s|$$

or

$$\dot{s} \leq -\eta \cdot sgn(s) \tag{3.7}$$

where η is a strictly positive constant. This equation states that the squared distance to the surface, as measured by s^2, decreases along all system state trajectories. Thus, it constrains trajectories to point towards the surface $S(t)$ and, once the state is on the surface, it remains on the surface. Because of this,

the inequality given by equation (3.7) is called the sliding condition. In fact, starting from any initial condition, the state trajectory reaches the surface $S(t)$ in a finite time smaller than $\left|S(t=0)\right|/\eta$, and then slides along the surface towards $\mathbf{x}_d$ exponentially, with a time-constant equal to $1/\lambda$. Furthermore, as will be shown, (3.7) also implies that some disturbances or dynamic uncertainties can be tolerated while keeping the surface on an invariant set.

To obtain the control law, let us differentiate the surface (3.6):

$$
\begin{aligned}
\dot{s}(\mathbf{x};t) &= \Lambda^T \dot{\mathbf{e}} \\
&= \Lambda_a{}^T \mathbf{e} + f + bu - x_d{}^{(n)}
\end{aligned}
\tag{3.8}
$$

where $\Lambda_a{}^T = \left(0, \lambda^{(n-1)}, \cdots, (n-1)\lambda\right)$. The dynamics $f(\mathbf{x})$ (possibly nonlinear or time-varying) is not exactly known, but estimated as a nominal function $\hat{f}(\mathbf{x})$. We assume that the estimation error on $f(\mathbf{x})$ is bounded by some known function $F = F(\mathbf{x})$:

$$
\left|\hat{f} - f\right| \le F
\tag{3.9}
$$

Thus, if we choose input u as

$$
u = \frac{1}{b}\left[-\hat{f} + x_d{}^{(n)} - \Lambda_a{}^T \mathbf{e} - k \cdot sgn(s)\right]
\tag{3.10}
$$

where $k = k(\mathbf{x}) = F + \eta$, then the sliding condition (3.7) may be satisfied.

In order to reduce the chattering effect, which results from using the $sgn(\cdot)$ function in the control law, a saturation function will be used in this report (Slotine and Li 1990).

When the system equation is not in the canonical form (i.e., it does not satisfy the matching condition defined as the nonlinearity and control input on same channel), a different approach is needed. In the case of non canonical form, we propose a method using multiple sliding surfaces instead of a single surface.

3.2.1.2 On-line parameter estimation for detecting road condition

In the vehicle traction control problem, the estimation error on $f(\mathbf{x})$ mainly depends on road conditions and can be very large when road conditions change widely (e.g. abrupt change from dry asphalt to icy road). If the magnitude of the estimation error on $f(\mathbf{x})$ is too large, even robust controllers such as the sliding mode controller fail to show an acceptable level of performance. They may show instability or results in too conservative control deteriorating performance. To deal with such a problem in vehicle traction control, we need to estimate the road condition during driving. We will develop an on-line road condition estimation scheme to improve the performance of the sliding mode controller. This estimated road condition will be used to adjust a parameter in the sliding mode control.

Simulation and experiment results strongly depend on the tire model to be used. In this research, we use the Bakker-Pacejka curve fitting model obtained based on the test data of a YOKOHAMA P205/60R 1487H steel-belt radial tire (Appendix E, Peng 1992). The set of curves in figure 3.1 represent fits based on tests from this tire as function of the slip ratio and the normal force ($F_z = 2000N$, 1500N, and 1000N).
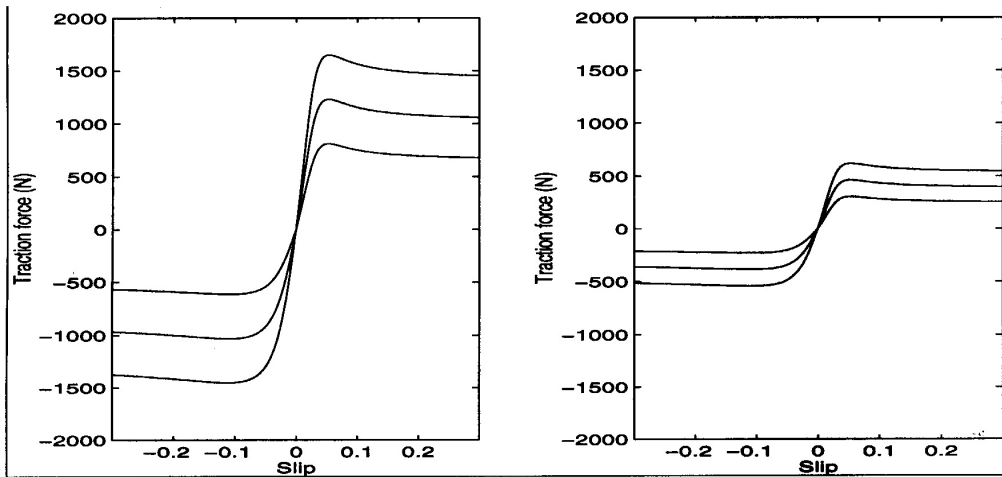
(a) Wet asphalt ($rc = 0.8$)   (b) Icy road ($rc = 0.3$)

Figure 3.1 Longitudinal traction force as function
of the slip ratio and the normal force

This tire model can be expressed by the relationship between traction force, tire slip, vertical force exerted at the tire, and the road condition: i.e.

$$F_x = rc \cdot fn(\lambda, F_z)$$ (3.11)

where rc denotes the road condition and takes values in the interval [0,1] depending on the road condition. Smaller values of rc correspond to more slippery road conditions. It should be noted that the peak slip value of this tire model is assumed to be fixed for the different road conditions (at 0.054 for acceleration and at -0.11 for deceleration). It is, however, an assumption not generally accepted as appropriate (Leiber and Czinczel 1983, Leiber et al. 1982, Wong 1978). Therefore, it is important to keep this restriction of the tire model in mind during designing the controller.

If we assume that the sum of the vertical loads exerted at each tire is equal to the static vehicle weight, we can consider normal force to be constant. Noting equation (2.2), the equation that describes longitudinal traction can be expressed as

$$\mu(x_3) = a_t \cdot f_t(x_3)$$ (3.12)

where $x_3 = \lambda$, $a_t = rc$, and $f_t(x_3) = \dfrac{fn(x_3, F_z)}{F_z}$. The parameter a_t is difficult to directly measure and must be estimated.

Problem formulation

Substituting (3.12) into (3.2), we have

$$\dot{x}_2 = -f_2(x_2) - a_t f_t(x_3) + b_3 T$$ (3.13)

Defining $y(t)$ as

$$y(t) = -\dot{x}_2 - f_2(x_2) + b_3 T$$ (3.14)

and assuming that we can measure angular acceleration ($\dot{x}_2$) and torque exerted at the wheel shaft (T) and that $f_2(x_2)$ can be treated as constant (the variability of $f_2(x_2)$ is very small), we can define $y(t)$ to be the "output" of the system. Then, (3.13) can be expressed in the form:

$$y(t) = a_t f_t(t)$$ (3.15)

Note that both $y(t)$ and $f_t(t)$ have been assumed to be known from the measurements of the system signals. Thus, the only unknown quantity in (3.15) is a_t. Our objective is to determine an adaptation law for estimating the parameter a_t, which depends on the road condition.

While the simplest approach for estimating a_t may appear to be dividing $y(t)$ by $f_t(t)$, it is not the best approach because $y(t)$ defined by equation (3.14) and $f_t(t)$ can not be accurate. Therefore, we use a least squares method. In off-line estimation, one collects the data of $y(t)$ and $f_t(t)$ for a period of time, and compute the least square estimate. In on-line recursive estimation, one solves the equation recursively, implying that the estimated value $\hat{a}_t$ is updated once a new set of data $y(t)$ and $f_t(t)$ becomes available.

Since the system has the following two properties,

(i)   parameter a_t is a time-varying parameter during driving due to time-varying road conditions and

(ii) measurements of $y(t)$ and $f_t(t)$ may be contaminated by noise,

we use a recursive least-squares scheme with a forgetting factor for estimation $\hat{a}_t$. This method has the capability of estimating time-varying parameter, and it is known to have good robustness with respect to noise and disturbance.

Least-squares estimation with exponential bounded-gain forgetting factor

The parameter estimate is generated by minimizing the integral prediction error with the exponential forgetting factor

$$J = \int_0^t exp\left[-\int_\tau^t \rho(r)dr\right]\left|y(\tau) - \hat{a}_t(t)f_t(\tau)\right|^2 d\tau \tag{3.16}$$

with respect to $\hat{a}_t(t)$, where $\rho(t) \geq 0$ is the time-varying forgetting factor. Note that the exponential term in the integral represents the weighting for the data. It discounts the influence of the past data in the estimation of the current parameter. This property is very useful in dealing with time-varying parameter.

The least squares estimate, $\hat{a}_t(t)$, satisfies

$$\left[\int_0^t exp\left[\int_\tau^t \rho(r)dr\right]f_t^2(\tau)d\tau\right]\hat{a}_t(t) = \int_0^t exp\left[\int_\tau^t \rho(r)dr\right]f_t(\tau)y(\tau)d\tau \tag{3.17}$$

Let

$$P(t) = \left[\int_0^t exp\left[-\int_\tau^t \rho(r)dr \right] f_t^2(\tau)d\tau \right]^{-1} \tag{3.18}$$

To achieve computational efficiency, it is desirable to compute $P(t)$ recursively, instead of evaluating the integral at every time instant. This amounts to replacing the above equation by the differential equation

$$\frac{d}{dt}\left[P^{-1}(t) \right] = -\rho(t)P^{-1}(t) + f_t(t)^2 \tag{3.19}$$

Differentiating (3.17) and using (3.18) and (3.19), we find that the parameter updating and gain updating equations given by

$$\dot{\hat{a}}_t = -P(t)f_t(t)e \tag{3.20}$$

$$\dot{P}(t) = \rho(t)P(t) - f_t(t)^2 P(t)^2 \tag{3.21}$$

with $P(t)$ being called the estimation gain. Since the magnitude of the gain $P(t)$ is an indicator of the excitation level of $f_t(t)$, it is reasonable to correlate the forgetting factor variation with $|P(t)|$. A specific technique for achieving this purpose is to choose

$$\rho(t) = \rho_o\left(1 - \frac{|P|}{k_o} \right) \tag{3.22}$$

with ρ_o and k_o being positive constants representing the maximum forgetting rate and pre-specified bound for gain matrix magnitude, respectively. The forgetting factor variation is tuned so that data forgetting is activated when $f_t(t)$ is persistently excited, and suspended when $f_t(t)$ is not. This means that the norm of the gain matrix has an upper bound, specified by the constant k_o, regardless of the persistence of excitation.

The estimation scheme developed here will be later introduced in the sliding mode controller (section 3.2.1.1) developed for the vehicle slip control in Section 3.3.1.1.

It is also noted that the least square scheme used in this work tends to introduce a bias error in the presence of measurement noise. Because the sliding control law is robust over a certain parameter range, such an error is assumed not to be critical.

3.2.2 Stable direct adaptive fuzzy logic controller (SDAFLC)

3.2.2.1 Description of fuzzy logic systems

We see in the conventional fuzzy logic literature that there are many different interpretations for the fuzzy IF-THEN rules which result in different mappings of the fuzzy inference engine (Lee 1990a , Lee 1990b, Pedrycz 1989). Also, we see that we have different types of fuzzifiers and defuzzifiers. Many combinations of these fuzzy inference engines, fuzzifiers, and defuzzifiers may constitute useful fuzzy logic systems. But we should consider computational efficiency and easiness for adaptation since we deal with on-line adaptive control problem. So, we may have to select a simpler fuzzy logic system which is linear in its adjustable parameters. As a result, we will consider a fuzzy logic system which is a combination of the product-inference rule, singleton fuzzifier, center average defuzzifier, and Gaussian membership function. The detailed functional forms of this fuzzy logic system is derived next.

Figure 3.2 shows the basic configuration of the standard fuzzy logic system considered in this report. The fuzzy logic system performs a mapping from $X \subset R^n$ to $U \subset R$.
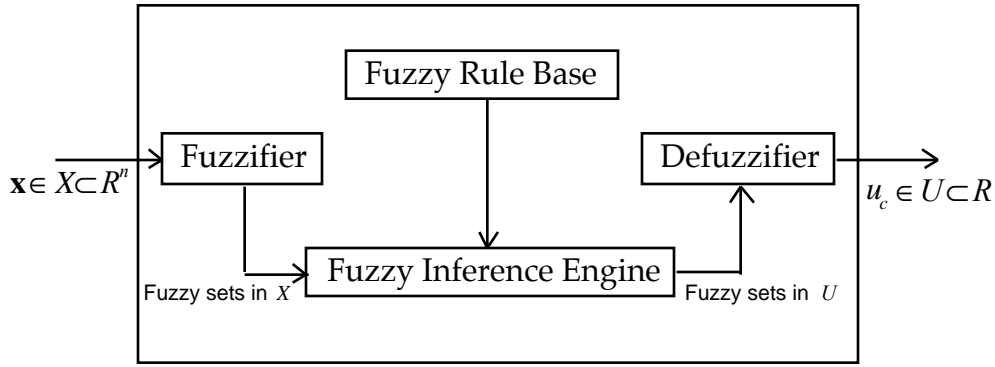

Figure 3.2 Basic configuration of fuzzy logic system

Fuzzy rule base

Fuzzy rule base consists of a collection of fuzzy IF-THEN rules:

$$R^{(l)}: IF \ \ x_1 \ \ is \ \ F_1^l \ \ and \cdots and \ x_n \ \ is \ \ F_n^l, \ \ Then \ \ u_c \ \ is \ \ G^l \tag{3.23}$$

where $\mathbf{x} = (x_1, \cdots, x_n)^T \in X$ and $u_c \in R$ are the input and output of the fuzzy logic system, respectively, F_i^l and G^l are labels of fuzzy sets in X_i and U, respectively, and $l = 1, 2, \cdots, M$. Each fuzzy IF-THEN rule defines a fuzzy implication $F_1^l \times \cdots \times F_n^l \rightarrow G^l$, which is a fuzzy set defined in the product space $X \times R$. Based on generalizations of implications in multivalue logic, many fuzzy implication rules have been proposed in the fuzzy logic literature. Here we will use the *Product-operation rule of fuzzy implication*:

$$\mu_{F_1^l \times \cdots \times F_n^l \rightarrow G^l}(\mathbf{x}, u_c) = \mu_{F_1^l \times \cdots \times F_n^l}(\mathbf{x}) \cdot \mu_{G^l}(u_c) \tag{3.24}$$

where $\mu_{F_1^l \times \cdots \times F_n^l}(\mathbf{x})$ is defined by

$$\mu_{F_1^l \times \cdots \times F_n^l}(\mathbf{x}) = \mu_{F_1^l}(x_1) * \cdots * \mu_{F_n^l}(x_n) \tag{3.25}$$

Here the symbol "$*$" denotes the *t-norm* (Lee 1990b), which corresponds to the conjunction "and" in (3.23). In this research, the algebraic product is used as t-norm

$$u * v = uv \tag{3.26}$$

Fuzzy inference engine

The fuzzy inference engine performs a mapping from fuzzy sets in X to fuzzy sets in R, based upon the fuzzy IF-THEN rules in the fuzzy rule base and the compositional rule of inference. Let A_x be an arbitrary fuzzy set in X; then, each $R^{(l)}$ of the fuzzy rule base determines a fuzzy set, $A_x \circ R^{(l)}$, in R based on the following sup-star compositional rule of inference:

$$\mu_{A_x \circ R^{(l)}} (u_c) = \sup_{\mathbf{x} \in X} \left[\mu_{A_x} (\mathbf{x}) * \mu_{F_1^l \times \cdots \times F_n^l \to G^l} (\mathbf{x}, u_c) \right] \tag{3.27}$$

where $*$ is the t-norm, and $\mu_{F_1^l \times \cdots \times F_n^l \to G^l} (\mathbf{x}, u_c)$ is determined by the fuzzy implication rules. If we use the product operation rule of fuzzy implication (3.24) and choose $*$ to be an algebraic product (3.26), then the inference is called product inference. Using product inference, (3.27) becomes

$$\mu_{A_x \circ R^{(l)}} (u_c) = \sup_{\mathbf{x} \in X} \left[\mu_{A_x} (\mathbf{x}) \mu_{F_1^l} (x_1) \cdots \mu_{F_n^l} (x_n) \mu_{G^l} (u_c) \right] \tag{3.28}$$

Fuzzifier

The fuzzifier maps a crisp point $\mathbf{x} = (x_1, \cdots, x_n)^T \in X$ into a fuzzy set A_x in E. Here we assume that A_x is a fuzzy singleton with support $\mathbf{x}$; i.e., $\mu_{A_x} (\mathbf{x}') = 1$ for $\mathbf{x}' = \mathbf{x}$ and $\mu_{A_x} (\mathbf{x}') = 0$ for $\mathbf{x}' \neq \mathbf{x}$.

Defuzzifier

The defuzzifier maps fuzzy sets in R to a crisp point in R. There are several possible choices of this mapping, and the *Center-average defuzzifier* is used in this report. Namely,

$$u_c = \frac{\sum_{l=1}^{M} \overline{u}_c^{\,l} \left(\mu_{A_x \circ R^{(l)}} \left(\overline{u}_c^{\,l} \right) \right)}{\sum_{l=1}^{M} \left(\mu_{A_x \circ R^{(l)}} \left(\overline{u}_c^{\,l} \right) \right)} \tag{3.29}$$

where $\overline{u}_c^{\,l}$ is the point in R at which $\mu_{G^l}(u_c)$ achieves its maximum value, and $\mu_{A_x \circ R^{(l)}} \left(u_c \right)$ is given by (3.28).

Lemma 1: The fuzzy logic system with *center-average defuzzifier* (3.29), *product inference* (3.28), and *singleton fuzzifier* are of the following form:

$$u_c(\mathbf{x}) = \frac{\sum_{l=1}^{M} \overline{u}_c^{\,l} \left(\prod_{i=1}^{n} \mu_{F_i^l}(x_i) \right)}{\sum_{l=1}^{M} \left(\prod_{i=1}^{n} \mu_{F_i^l}(x_i) \right)} \tag{3.30}$$

where $\overline{u}_c^{\,l}$ is the point at which $\mu_{G^l}(u_c)$ achieves its maximum value, and we assume that $\mu_{G^l}\left(\overline{u}_c^{\,l} \right) = 1$.

Proof: If we use the singleton fuzzifier, we have $\mu_{A_x}(\mathbf{x}') = 1$ for $\mathbf{x}' = \mathbf{x}$ and $\mu_{A_x}(\mathbf{x}') = 0$ for all other $\mathbf{x}' \in X$ ($\mathbf{x}$ is the input crisp point to the fuzzy logic controller) ; therefore, the "sup" in (3.28) is achieved at $\mathbf{x}' = \mathbf{x}$, and (3.28) can be simplified to

$$\mu_{A_x \circ R^{(l)}} \left(\overline{u}_c^{\,l} \right) = \prod_{i=1}^{n} \mu_{F_i^l}(x_i) \tag{3.31}$$

Substituting (3.31) into (3.29), we obtain (3.30). Q.E.D.

If we fix the $\mu_{F_i^l}(x_i)$'s and view the $\overline{u}_c^{\,l}$'s as adjustable parameters, then (3.30) can be written as

$$u_c(\mathbf{x}|\Theta) = \sum_{l=1}^{M} \overline{u}_c^{\ l} \xi^l(\mathbf{x})$$

$$= \Theta^T \Xi(\mathbf{x}) \tag{3.32}$$

where $\Theta = \left(\overline{u}_c^{\ 1}, \cdots, \overline{u}_c^{\ M}\right)^T$ is a parameter vector which is the collection of the points at which $\mu_{G^l}(u_c)$'s achieves its maximum value, M is the number of rules in the rule base, $\Xi(\mathbf{x}) = \left(\xi^1(\mathbf{x}), \cdots, \xi^M(\mathbf{x})\right)^T$, and $\xi^l(\mathbf{x})$'s are the fuzzy basis functions (FBF's, Wang and Mendel 1992) defined by

$$\xi^l(\mathbf{x}) = \frac{\prod_{i=1}^{n} \mu_{F_i^l}(x_i)}{\sum_{l=1}^{M}\left(\prod_{i=1}^{n} \mu_{F_i^l}(x_i)\right)} \tag{3.33}$$

Clearly, equation (3.32) is equivalent to equation (3.30) assuming that $\mu_{F_i^l}(x_i)$'s are given; i.e., $\mu_{F_i^l}(x_i)$ will not change during the adaptation (training) procedure. Our first choice for the membership function is the following Gaussian function:

$$\mu_{F_i^l}(x_i) = a_i^{\ l} \, exp\left(-\left(\frac{x_i - \overline{x}_i^{\ l}}{\sigma_i^{\ l}}\right)^2\right) \tag{3.34}$$

where $a_i^{\ l}$, $\overline{x}_i^{\ l}$, and $\sigma_i^{\ l}$ are adjustable parameters.

Lemma 2 : The fuzzy logic systems (3.30) with Gaussian membership function (3.34) are of the following form:

$$u_c(\mathbf{x}|\Theta) = \frac{\sum_{l=1}^{M} \overline{u}_c^{\ l}\left(\prod_{i=1}^{n} a_i^{\ l} \, exp\left(-\left(\frac{x_i - \overline{x}_i^{\ l}}{\sigma_i^{\ l}}\right)^2\right)\right)}{\sum_{l=1}^{M}\left(\prod_{i=1}^{n} a_i^{\ l} \, exp\left(-\left(\frac{x_i - \overline{x}_i^{\ l}}{\sigma_i^{\ l}}\right)^2\right)\right)} \tag{3.35}$$

Proof : Just substitute equation (3.34) into (3.30)

3.2.2.2 Basic ideas of constructing SDAFLC

When the fuzzy logic system described above is used as a controller, they are called a fuzzy logic controller. Fuzzy logic controllers are supposed to work in situations where there is a large uncertainty or unknown variation in plant parameters and structures. Generally, the basic objective of adaptive control is

to maintain consistent performance of a system in the presence of these uncertainties. Therefore, advanced fuzzy control should be adaptive.

In the conventional adaptive control literature, adaptive controllers are classified into two categories (Narendra and Parthasarathy 1990, Narendra and Annaswamy 1989): direct and indirect adaptive controllers. Formally, we have the following definition for the adaptive fuzzy logic controllers:

(i)   If an adaptive fuzzy controller uses adaptive fuzzy logic systems, which are equipped with a adaptation algorithm, as controllers, it is called a direct adaptive fuzzy logic controller. A direct adaptive fuzzy logic controller can incorporate fuzzy control rules directly into itself.
(ii) If an adaptive fuzzy controller uses adaptive fuzzy logic systems as a model of the plant, it is called an indirect adaptive fuzzy logic controller. An indirect adaptive fuzzy logic controller can incorporate fuzzy descriptions of the plant (in terms of fuzzy IF-THEN rules) directly into itself.

In this report, we will consider a direct adaptive fuzzy logic controller which can be successfully derived with proven stability (Wang 1993).

Consider an nth-order nonlinear system of the canonical form

$$x^{(n)} = f\left(x, \dot{x}, \cdots, x^{(n-1)}\right) + bu, \qquad y = x \tag{3.36}$$

where f is an unknown continuous function, and $u \in R$ and $y \in R$ are the input and output of the system, respectively.

Assumption : We can determine a function $f^{U}(\mathbf{x})$ such that $\left|f(\mathbf{x})\right| \leq f^{U}(\mathbf{x})$.

This assumption means the plant (3.36) can be viewed as "poorly-understood," but not "totally unknown." Note that in this assumption we need to know the state-dependent bounds of f, which is less restrictive than requiring fixed bounds for all $\mathbf{x} \in X$. This system formulation with the above assumptions is appropriate to address the traction control problem where the road condition is unknown during driving. In fact, equation (3.3) is the same as (3.36) when $n = 1$.

Control objectives: Determine a feedback control $u = u(\mathbf{x}|\Theta)$ and an adaptive law for adjusting the parameter vector Θ such that the following conditions are met:

(i)   The closed-loop system must be globally stable in the sense that all variables ($\mathbf{x}(t), \Theta(t), u(\mathbf{x}|\Theta)$) must be uniformly bounded; i.e., $\left|\mathbf{x}(t)\right| \leq M_x < \infty$, $\left|\Theta(t)\right| \leq M_\theta < \infty$, and $\left|u(\mathbf{x}|\Theta)\right| \leq M_u < \infty$ for all $t \geq 0$.
(ii) The tracking error, $e \equiv x_d - x$, should be as small as possible under the constraints in (i).

We now show the basic ideas of how to construct a direct adaptive fuzzy controller to achieve these control objectives.

Let $\mathbf{e} = \left(e, \dot{e}, \cdots, e^{(n-1)}\right)^T$ and $\mathbf{k} = \left(k_n, \cdots, k_1\right)^T$ be such that all roots of the polynomial $h(s) = s^n + k_1 s^{n-1} + \cdots + k_n$ are in the open left-half plane. If the function $f(\mathbf{x})$ is known, then the control law

$$u^* = \frac{1}{b}\left[-f(\mathbf{x}) + x_d^{(n)} + \mathbf{k}^T \mathbf{e}\right] \tag{3.37}$$

applied to (3.36) results in

$$e^{(n)} + k_1 e^{(n-1)} + \cdots + k_n e = 0 \tag{3.38}$$

which implies that $\lim\limits_{t \to \infty} e(t) = 0$ - the main objective of control. Since $f(\mathbf{x})$ is unknown, the optimal control, u^* cannot be implemented. Our purpose is to design a fuzzy logic control to approximate this optimal control.

The following theorem shows that the fuzzy logic systems in Lemma 2 are capable of uniformly approximating any nonlinear function over X to any degree of accuracy if X is compact (Wang and Mendel 1992). Let Y be the set of all the FBF expansions (3.35) with FBF's given by (3.33) and (3.34), and $d_\infty(f_1, f_2) = \sup\limits_{\mathbf{x} \in X} |f_1(x) - f_2(x)|$ be the sup-metric; then, (Y, d_∞) is a metric space (Rudin 1976).

Theorem 1: (Universal Approximation Theorem)

For any given real continuous function u^* on a compact set $X \in R^n$ and arbitrary $\varepsilon > 0$, there exist a fuzzy logic system $u_c \in Y$ in the form of (3.35) such that $d_\infty(u_c, u^*) = \sup\limits_{\mathbf{x} \in X} |u_c(\mathbf{x}|\Theta^*) - u^*(\mathbf{x})| < \varepsilon$.

Proof : A proof of this theorem is given in appendix A.

We make a few remarks on this Universal Approximation Theorem.

(i) While many other types of functions are also universal approximators, including the simple polynomials, neural networks with sigmoidal functions, etc., it is shown in (Poggio and Girosi 1990) that Gaussian basis functions have the best approximation property. This is the main reason we choose the Gaussian functions as the membership functions.

(ii) In this theorem, Θ^* means the optimal parameter vector of Θ. An adaptive law for the parameter vector Θ to approximate Θ^* will be developed next.

(iii) When the initial value of Θ is not chosen adequately, or Θ^* is changed due to changing system properties, the difference between Θ^* and Θ becomes large. This large difference will cause system instability or long transient time.

Suppose that the control u is the summation of a fuzzy control $u_c(\mathbf{x}|\Theta)$ and a supervisory control $u_s(\mathbf{x})$:

$$u = u_c(\mathbf{x}|\Theta) + u_s(\mathbf{x}) \tag{3.39}$$

where a supervisory control $u_s(\mathbf{x})$ is introduce from the consideration of remark (iii) in order to provide stability and fast response. Our purpose is to construct a fuzzy control $u_c(\mathbf{x}|\Theta)$ by developing an adaptive law for the parameter vector Θ, and a supervisory control $u_s(\mathbf{x})$ which will guarantee stability of the closed loop system.

3.2.2.3 Constructing $u_s(\mathbf{x})$ (Wang 1993)

Substituting (3.39) into (3.36), we have

$$x^{(n)} = f(\mathbf{x}) + b[u_c(\mathbf{x}|\Theta) + u_s(\mathbf{x})] \tag{3.40}$$

Now adding and subtracting bu^* to (3.40), we obtain an error equation governing the closed-loop system. i.e.,

$$e^{(n)} = -\mathbf{k}^T\mathbf{e} + b\left[u^* - u_c\left(\mathbf{x}|\Theta\right) - u_s\left(\mathbf{x}\right)\right] \tag{3.41}$$

or, equivalently,

$$\dot{\mathbf{e}} = \Lambda_c\mathbf{e} + \mathbf{b}_c\left[u^* - u_c\left(\mathbf{x}|\Theta\right) - u_s\left(\mathbf{x}\right)\right] \tag{3.42}$$

where

$$\Lambda_c = \begin{bmatrix} 0 & 1 & 0 & 0 & \cdot & 0 & 0 \\ 0 & 0 & 1 & 0 & \cdot & 0 & 0 \\ \cdot & \cdot & \cdot & \cdot & \cdot & \cdot & \cdot \\ 0 & 0 & 0 & 0 & \cdot & 0 & 1 \\ -k_n & -k_{n-1} & \cdot & \cdot & \cdot & & -k_1 \end{bmatrix}, \quad \mathbf{b}_c = \begin{bmatrix} 0 \\ \cdot \\ 0 \\ b \end{bmatrix} \tag{3.43}$$

Define $V_e = \dfrac{1}{2}\mathbf{e}^T\mathbf{P}\mathbf{e}$, where $\mathbf{P}$ is a symmetric positive definite matrix satisfying the Lyapunov equation

$$\Lambda_c^T\mathbf{P} + \mathbf{P}\Lambda_c = -\mathbf{Q} \tag{3.44}$$

where $\mathbf{Q} > 0$.

Using (3.42) and (3.44), V_e can be differentiated with respect to time to obtain

$$\dot{V}_e = -\frac{1}{2}\mathbf{e}^T\mathbf{Q}\mathbf{e} + \mathbf{e}^T\mathbf{P}\mathbf{b}_c\left[u^* - u_c(\mathbf{x}|\Theta) - u_s(\mathbf{x})\right]$$

$$\leq -\frac{1}{2}\mathbf{e}^T\mathbf{Q}\mathbf{e} + \left|\mathbf{e}^T\mathbf{P}\mathbf{b}_c\right|\left(\left|u^*\right| + \left|u_c(\mathbf{x}|\Theta)\right|\right) - \mathbf{e}^T\mathbf{P}\mathbf{b}_c u_s(\mathbf{x}) \tag{3.45}$$

If $u_c(\mathbf{x}|\Theta)$ approximates $u_c(\mathbf{x}|\Theta^*)$ (i.e., u^*), u_s is not necessary to make $\dot{V}_e \leq 0$. Our task now is to design u_s such that $\dot{V}_e \leq 0$ always.

We construct the supervisory control $u_s(\mathbf{x})$ as follows:

$$u_s(\mathbf{x}) = I_1^* sgn(\mathbf{e}^T\mathbf{P}\mathbf{b}_c)\left[\left|u_c\right| + \frac{1}{b}\left(f^U + \left|x_d^{(n)}\right| + \left|\mathbf{k}^T\mathbf{e}\right|\right)\right] \tag{3.46}$$

where $I_1^* = 1$ if $V_e > \overline{V}$, and $I_1^* = 0$ if $V_e \leq \overline{V}$ ($\overline{V}$ is a constant specified by the designer).

Substituting (3.46) to (3.45) and considering the case where $I_1^* = 1$, we have

$$\dot{V}_e \leq -\frac{1}{2}\mathbf{e}^T\mathbf{Q}\mathbf{e} + \left|\mathbf{e}^T\mathbf{P}\mathbf{b}_c\right|\left(\frac{1}{b}\left(\left|f\right| + \left|x_d^{(n)}\right| + \left|\mathbf{k}^T\mathbf{e}\right|\right) - \frac{1}{b}\left(f^U + \left|x_d^{(n)}\right| + \left|\mathbf{k}^T\mathbf{e}\right|\right)\right)$$

$$\leq -\frac{1}{2}\mathbf{e}^T\mathbf{Q}\mathbf{e} \leq 0 \tag{3.47}$$

Therefore, using the supervisory control u_s, we always have $V_e \leq \overline{V}$.

From (3.46) we see that the u_s is nonzero only when $V_e > \overline{V}$. That is, if the pure fuzzy control $u_c(\mathbf{x}|\Theta)$ approximate very close to $u_c(\mathbf{x}|\Theta^*)$ (i.e. to u^*) and, so, the closed-loop system with $u_c(\mathbf{x}|\Theta)$ is well behaved in the sense that the error is not big (i.e., $V_e \leq \overline{V}$), then the supervisory control

u_s is zero. On the other hand, if the system tends to be unstable (i.e., $V_e > \overline{V}$), then the supervisory control u_s begins operating to force $V_e \leq \overline{V}$. In this way, the control u_s is like a *supervisor*; this is why we call u_s a supervisory control.

3.2.2.4 Developing an adaptive law for the parameter vector Θ

We replace the $u_c(\mathbf{x}|\Theta)$ by the fuzzy logic control given by (3.32) and develop an adaptive law to adjust the parameter vector Θ. Define the optimal parameter vector:

$$\Theta^* \equiv \underset{|\Theta| \leq M_\theta}{arg\,min} \left[\underset{|\mathbf{x}| \leq M_x}{sup} \left| u_c(\mathbf{x}|\Theta) - u^* \right| \right] \tag{3.48}$$

and the "minimum approximation error":

$$w \equiv u_c(\mathbf{x}|\Theta^*) - u^* \tag{3.49}$$

The error equation (3.42) can be rewritten as

$$\begin{aligned}
\dot{\mathbf{e}} &= \Lambda_c \mathbf{e} + \mathbf{b}_c \left[u_c(\mathbf{x}|\Theta^*) - u_c(\mathbf{x}|\Theta) \right] - \mathbf{b}_c u_s(\mathbf{x}) - \mathbf{b}_c w \\
&= \Lambda_c \mathbf{e} + \mathbf{b}_c \Phi^T \Xi(\mathbf{x}) - \mathbf{b}_c u_s - \mathbf{b}_c w
\end{aligned} \tag{3.50}$$

where $\Phi \equiv \Theta^* - \Theta$ and $\Xi(\mathbf{x})$ is the vector of FBF's. Define a Lyapunov function candidate

$$V = \frac{1}{2} \mathbf{e}^T \mathbf{P} \mathbf{e} + \frac{b}{2\gamma} \Phi^T \Phi \tag{3.51}$$

Using (3.50) and (3.44), we have

$$\dot{V} = -\frac{1}{2} \mathbf{e}^T \mathbf{Q} \mathbf{e} + \mathbf{e}^T \mathbf{P} \mathbf{b}_c \left[\Phi^T \Xi(\mathbf{x}) - u_s - w \right] + \frac{b}{\gamma} \Phi^T \Phi \tag{3.52}$$

Let $\mathbf{p}_n$ be the last column of $\mathbf{P}$; then we have

$$\mathbf{e}^T \mathbf{P} \mathbf{b}_c = \mathbf{e}^T \mathbf{p}_n b \tag{3.53}$$

Substituting (3.53) into (3.52), we have

$$\dot{V} = -\frac{1}{2}\mathbf{e}^T\mathbf{Q}\mathbf{e} + \frac{b}{\gamma}\Phi^T\left[\gamma\mathbf{e}^T\mathbf{p}_n\Xi(\mathbf{x}) + \dot{\Phi}\right] - \mathbf{e}^T\mathbf{Pb}_c u_s - \mathbf{e}^T\mathbf{Pb}_c w \tag{3.54}$$

If we choose the adaptive law:

$$\dot{\Theta} = \gamma\mathbf{e}^T\mathbf{p}_n\Xi(\mathbf{x}) \qquad \text{if } (|\Theta| < M_\theta) \text{ or } (|\Theta| = M_\theta \quad and \quad \mathbf{e}^T\mathbf{p}_n\Theta^T\Xi(\mathbf{x}) \leq 0) \tag{3.55}$$

$$\dot{\Theta} = \gamma\mathbf{e}^T\mathbf{p}_n\Xi(\mathbf{x}) - \gamma\mathbf{e}^T\mathbf{p}_n\frac{\Theta\Theta^T\Xi(\mathbf{x})}{|\Theta|^2} \qquad \text{if } |\Theta| = M_\theta \quad and \quad \mathbf{e}^T\mathbf{p}_n\Theta^T\Xi(\mathbf{x}) > 0 \tag{3.56}$$

where M_θ is a constant specified by the designer. Substituting (3.55) into (3.54), we have

$$\dot{V} \leq -\frac{1}{2}\mathbf{e}^T\mathbf{Q}\mathbf{e} - \mathbf{e}^T\mathbf{Pb}_c w \tag{3.57}$$

where we use the facts $\mathbf{e}^T\mathbf{Pb}_c u_s \geq 0$ and $\dot{\Phi} = -\dot{\Theta}$. This is the best we can achieve. From Universal Approximation Theorem, we have $\sup_{\mathbf{x}\in X}|w(\mathbf{x})| < \varepsilon$ for arbitrary $\varepsilon > 0$. If $w = 0$, that is, the searching space for $u_c\left(\mathbf{x}|\Theta^*\right)$ is so big that the u^* is included in them, then we have $\dot{V} \leq 0$. Even though it is not equal to zero, we can expect that the w should be small enough to get $\dot{V} \leq 0$, provided that we use sufficiently complex $u_c\left(\mathbf{x}|\Theta^*\right)$ (in terms of number of adjustable parameters). In order to guarantee $|\Theta| \leq M_\theta$, we use a projection algorithm as given (3.55) and (3.56) [19].

The following theorem shows the properties of this direct adaptive fuzzy logic controller.

Theorem 2 : Consider the nonlinear plant (3.36) with control (3.39), where $u_c\left(\mathbf{x}|\Theta\right)$ is given by (3.32), u_s is given by (3.46), and the parameter vector Θ is adjusted by the adaptive law (3.55) or (3.56). Then, the overall control scheme guarantees the following properties:

(i) $$|\Theta| \leq M_\theta \tag{3.58}$$

$$|\mathbf{x}(t)| \leq |\mathbf{x}_d| + \left(\frac{2\bar{V}}{\lambda_{min}}\right)^{1/2} \tag{3.59}$$

$$|u(t)| \leq 2M_\theta + \frac{1}{b}\left[f^U + \left|x_d^{(n)}\right| + |k|\left(\frac{2\bar{V}}{\lambda_{min}}\right)^{1/2}\right] \tag{3.60}$$

for all $t \geq 0$, where λ_{min} is the minimum eigenvalue of P, and

$$\mathbf{x}_d = \left(x_d, \dot{x}_d, \cdots, x_d^{(n-1)}\right)^T.$$

(ii) $$\int_0^t |\mathbf{e}(\tau)|^2 d\tau \leq a + c\int_0^t |w(\tau)|^2 d\tau \tag{3.61}$$

for all $t \geq 0$, where a and c are constants, and w is the minimum approximation error defined by (3.49).

(iii)   If w is squared integrable, i.e., $\int_0^\infty \left| w(t) \right|^2 dt < \infty$, then $\lim_{t \to \infty} \left| \mathbf{e}(t) \right| = 0$.

***Proof* :** A proof of this theorem is given in appendix B.

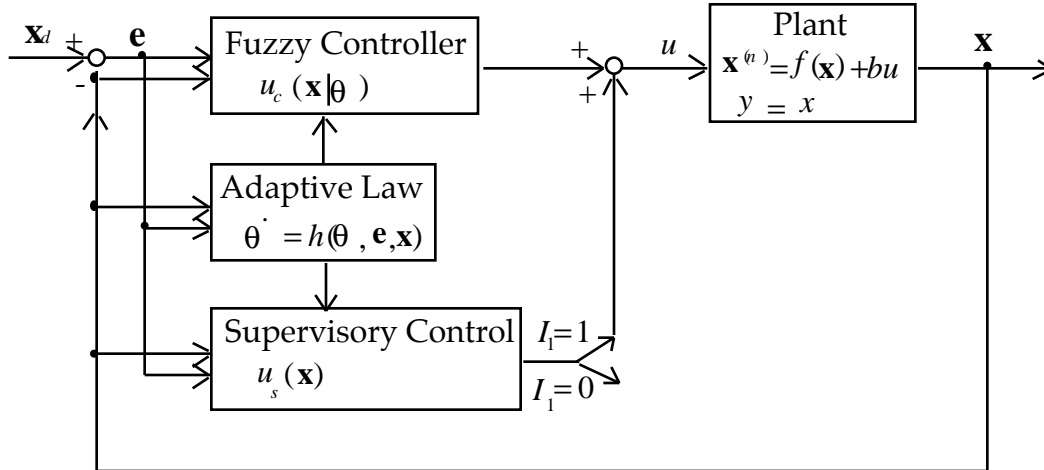To summarize, the overall scheme of our direct adaptive fuzzy controller is shown in figure 3.3.

Figure 3.3 The overall scheme of direct adaptive fuzzy control

3.3 Applications and simulations

Vehicle velocity (v_v) and wheel angular velocity (w_w) are assumed to be measured exactly. The wheel angular velocity is measured by a tachometer, and the vehicle velocity is measured by measuring the number of *magnetic markers* which are swept during a certain period of time or timing the travel time from one marker to the next. Measurement noise is not considered in simulation.

The tire model obtained in (3.12) is assumed as the real tire model. Analytical approximation of the real road conditions can be denoted as

Dry asphalt: $rc = 0.8$
wet asphalt: $rc = 0.5$
Icy road   : $rc = 0.3$

The vehicle parameters for simulation are

$M_V = 1000$ kg
$R_W = 0.31$ m
$F_z = 2450$ N
$n_w = 2$ for acceleration, 4 for deceleration
$J_W = 1.11$ $kg \cdot m^2$
$f_1(x_1) = c_w (R_w x_1 + wind\_gust)^2$ $c_w = 0.45 / (M_v R_w)$
$f_2(x_2) = 0.0$

From the data, the following parameter values are calculated

$b_1 = 15.81$ for acceleration, 31.62 for deceleration
$b_2 = 684.24$
$b_3 = 0.91$

The system parameters, b_1, b_2, b_3,, and f_1, are assumed to have a 25 % uncertainty range around the nominal values. The sampling frequency in the simulation is 1 kHz.

We define five fuzzy sets over interval [-2,2], with labels NB (negative big), NS (negative small), ZO (zero), PS (positive small), PB (positive big) which are shown in figure 3.4. Fuzzy membership functions for these labels are

$$\mu_{NB} = \frac{1}{1 + e^{5(x+1)}} \quad \mu_{NS} = e^{-(x+1)^2} \quad \mu_{ZO} = e^{-(x+0)^2} \quad \mu_{PS} = e^{-(x-1)^2} \quad \mu_{PB} = \frac{1}{1 + e^{-5(x-1)}}$$
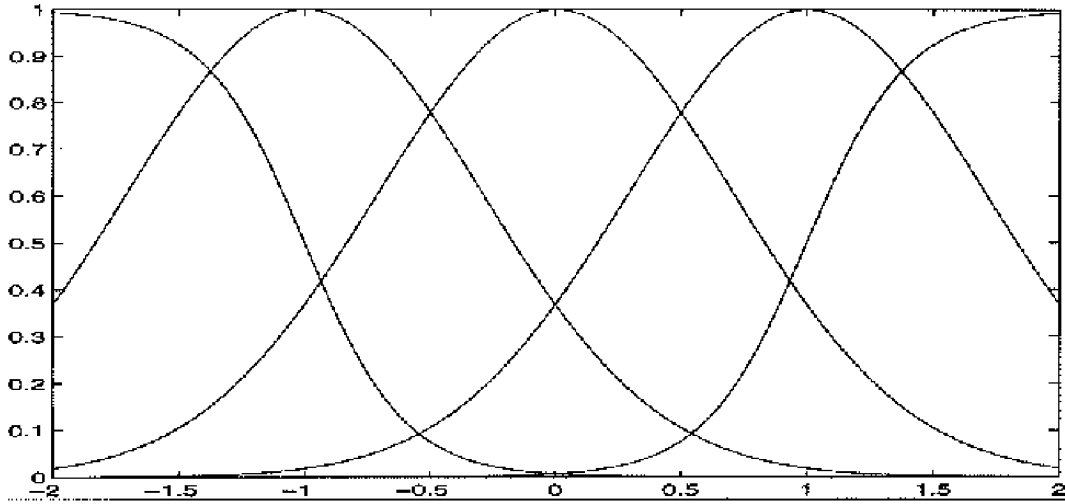
Figure 3.4 Fuzzy membership functions defined over the state space

Since the state x_3 is required to be constrained within the stable region (positive slope region at $\mu - \lambda$ curve), we choose $M_x = 0.15$. (Here, we do not choose M_x as the peak slip value since we do not want to use high gain control u_s frequently.) We also choose $M_u = 1000$ by considering possible engine torque. Since we know $f^U = 1$ and $|x_d| = 0.04$ (This $|x_d|$ value will be changed at each control objective.), based on equations (3.59) and (3.60), we can specify the design parameters as

$$Q = 2, \quad P = 1, \quad k = 1, \quad \bar{V} = 0.02, \quad M_\theta = 100 M_y = 450, \quad \gamma = 100$$

3.3.1 Slip Control

One of the main objectives of the vehicle traction control is the slip control. Slip control means regulating wheel slip at any desired value that is required for the minimum time control, the longitudinal platoon control, and the maximum steerability in lateral control.

3.3.1.1 Sliding mode controller

The wheel slip dynamic equation can be written as

$$\dot{\lambda} = f_3(x_1, x_2) - f_4(\lambda)\mu(\lambda) + f_5(\lambda)T \tag{3.62}$$

where $\lambda = x_3$. The sliding surface is defined as

$$s(t) = \lambda_e(t) = 0 \tag{3.63}$$

where $\lambda_e = \lambda - \lambda_{des}$, and λ_{des} is the desired wheel slip. In order to derive the control input, we differentiate this surface with respect to time:

$$\dot{s} = \dot{\lambda} - \dot{\lambda}_{des} \tag{3.64}$$

Substituting in the slip dynamic equation (3.3) and inserting sliding condition (3.7) yields:

$$\dot{s} = f_3(x_1, x_2) - f_4(\lambda)\mu(\lambda) + f_5(\lambda)T - \dot{\lambda}_{des} = -\eta sat\left(\frac{s}{\Phi}\right) \tag{3.65}$$

Solving this equation for T, we can obtain the control input.

$$T = \frac{1}{f_5(\lambda)}\left(-f_3(x_1, x_2) + f_4(\lambda)\mu(\lambda) + \dot{\lambda}_{des} - \eta sat\left(\frac{s}{\Phi}\right)\right) \tag{3.66}$$

To avoid chattering, a continuous approximation using a saturation function for the boundary layer has been used instead of the sign function in equations (3.65) and (3.66). It is defined by

$$\eta sat\left(\frac{s}{\Phi}\right) = \frac{s}{\Phi} \qquad for \ \ |s| \leq \Phi$$
$$= sgn(s) \qquad for \ \ |s| > \Phi \tag{3.67}$$

where Φ is the fixed boundary layer width and is chosen after careful consideration of the frequency range of the unmodelled dynamics.

To determine input torque, T, it is necessary to know $\mu(\lambda)$. For the standard sliding mode control (SSMC, without road condition estimation), the parameter $a_t(t)$ in equation (3.12) is assumed to be 0.45 which is a mean value of two extreme values (0.8 for dry asphalt and 0.3 for icy road) to obtain a nominal $\mu(\lambda)$. For the adaptive sliding mode control (ASMC, with road condition estimation), this $\mu(\lambda)$ is replaced by $\hat{\mu}(\lambda) = \hat{a}_t(t)f(\lambda)$ and $\hat{a}_t(t)$ is estimated utilizing the scheme developed in 3.2.1.2.

3.3.1.2 Fuzzy logic controller

Standard fuzzy logic controller (SFLC):

λ_e and $\dot{\lambda}_e$ are chosen as the input fuzzy variables for the fuzzy logic wheel slip control. Twenty five fuzzy control rules are derived by engineering judgment (table 1). For example, if λ_e is positive (PB or PS) and keeps increasing ($\dot{\lambda}_e$ = PB

or PS), then the input torque should be decreased (T= NB or NS). Note that increasing total input torque makes the slip increase.

Table 1 Fuzzy rule table for SFLC

		λ_e				
		NB	NS	ZO	PS	PB
$\dot{\lambda}_e$	NB	PB	PB	PS	NS	NS
	NS	PB	PB	PS	NS	NS
	ZO	PB	PS	ZO	NS	NB
	PS	PS	PS	NS	NB	NB
	PB	PS	PS	NS	NB	NB

Since we use symmetric Gaussian membership functions and the center-average defuzzifier, each fuzzy variable of THEN part can be denoted by singletons such as NB=-2, NS=-1, ZO=0, PS=1, PB=2.

Adaptive fuzzy logic controller (AFLC) :

Since the consequence of each fuzzy control rule, $\theta_i = \bar{u}_c^{\ i}$, may be adjusted by the adaptation scheme, the fuzzy rule base is formulated as in table 2.

We will consider two cases:

i) Without initial fuzzy control rule (AFLC0): There are no fuzzy control rules. Therefore, the initial $\bar{u}_c^{\ i}$'s are chosen randomly in the interval [-2,2], say zero.

ii) With initial fuzzy control rule (AFLC1): There are twenty five fuzzy control rules which are the same as those of SFLC. Therefore, every initial $\bar{u}_c^{\ i}$ has the same value as shown in table 1.

Table 2 fuzzy rule table For AFLC

		λ_e				
		NB	NS	ZO	PS	PB
$\dot{\lambda}_e$	NB	$\bar{u}_c^{\ 1}$	$\bar{u}_c^{\ 2}$	$\bar{u}_c^{\ 3}$	$\bar{u}_c^{\ 4}$	$\bar{u}_c^{\ 5}$
	NS	$\bar{u}_c^{\ 6}$	$\bar{u}_c^{\ 7}$	$\bar{u}_c^{\ 8}$	$\bar{u}_c^{\ 9}$	$\bar{u}_c^{\ 10}$
	ZO	$\bar{u}_c^{\ 11}$	$\bar{u}_c^{\ 12}$	$\bar{u}_c^{\ 13}$	$\bar{u}_c^{\ 14}$	$\bar{u}_c^{\ 15}$
	PS	$\bar{u}_c^{\ 16}$	$\bar{u}_c^{\ 17}$	$\bar{u}_c^{\ 18}$	$\bar{u}_c^{\ 19}$	$\bar{u}_c^{\ 20}$
	PB	$\bar{u}_c^{\ 21}$	$\bar{u}_c^{\ 22}$	$\bar{u}_c^{\ 23}$	$\bar{u}_c^{\ 24}$	$\bar{u}_c^{\ 25}$

3.3.1.3 Simulation results (figures 3.6, 3.7, 3.8, 3.9, 3.10, and 3.11)

Figure 3.6 shows the results of SFLC (without adaptation algorithm) and AFLC. The road condition is changed at $t = 1$sec from dry asphalt to icy road. As shown in this figure, performance is obviously improved by using the adaptation algorithm. SFLC exhibits a steady state error due to an inexact rule base, and is not robust to changes in road conditions and vehicle parameters, or to different driving conditions. The results also show that the presence of initial rules in AFLC enhances system performance at the initial stages. As adaptation is continued for a long time, however, we note that the results of the AFLC0 case converges to that of the AFLC1 case. For convenience in the graphical figures, the controller parameter values (y_i) are defined to be equal to $\bar{u}_c^i$ scaled down by a factor of 100. They are shown in figure 3.7 and figure 3.8 for each case to provide some idea about the transient response. Actual numerical values and the correspondence between parameters and plots are not important. As shown in figure 3.8, the parameter values are initialized to zero in the AFLC0 case. Figure 3.9 shows the results for each case when the desired slip is abruptly changed.

Figure 3.10 shows the comparison of the adaptive fuzzy control with initial rules (AFLC1) and the sliding mode control with/without road condition estimation (ASMC / SSMC). The performance of both the SMC and the FLC heavily depend on the control gains. In this simulation, the control gains are set so that the input torque of each controller has the same level. The SSMC shows poor results. It shows steady state error, and is not robust to road condition change, while the ASMC shows good performance compared with the AFLC1. Figure 3.11 shows parameter convergence and robustness to noise of the least-squares estimation with exponential bounded gain forgetting factor for road condition estimation.

3.3.2 Minimum time control
(minimum time acceleration or deceleration)

The minimum time control means achieving the fastest acceleration and the fastest deceleration, and this implies maximizing the magnitude of the traction force. These maximum traction forces are achieved at the positive or negative peak point of the $\mu - \lambda$ curve. Therefore, to produce the fastest acceleration, the wheel slip should be regulated where the adhesion coefficient attains the peak value. Since the peak value of λ varies depending on the tire characteristics, the road condition, and the normal force exerted at the tire, it is unknown during driving in general case. Therefore, the minimum time control includes searching for and maintaining the peak slip.

3.3.2.1 Sliding mode controller

The proposed method of the minimum time control contains the following three basic steps.

(i)   Estimate the local slope in the $\mu - \lambda$ curve
(ii) Move the target slip in the estimated direction towards the peak slip
(iii) Steer the wheel slip toward the new target slip via the sliding mode slip traction control and then return to (i).

Estimation of the local slope

In practice, the adhesion coefficient can be regarded as a function of time (since road condition is changed) and of slip. Under the assumption that the road condition changes, $\dfrac{\partial \mu}{\partial \lambda}$ can be approximated by

$$\frac{\partial \mu}{\partial \lambda}(t_k) \approx \frac{d\mu}{d\lambda}(t_k) \approx \frac{\Delta\mu(t_k)}{\Delta\lambda(t_k)} \tag{3.68}$$

where $\Delta\mu(t_k)$ and $\Delta\lambda(t_k)$ are the differences between the adjacent sampling instants. To obtain the value of $\Delta\mu(t_k)$, we differentiate (2.6) with respect to time and rearrange terms.

$$\frac{\partial \mu}{\partial \lambda} = \frac{\partial \mu}{\partial t}\frac{\partial t}{\partial \lambda} = \left(\ddot{x}_1 + \frac{\partial f_1}{\partial x_1}\dot{x}_1 \right)\frac{1}{b_1 \dot{\lambda}} \approx \frac{\Delta\hat{\mu}}{\Delta\hat{\lambda}} \tag{3.69}$$

Since the second term inside the bracket is usually insignificant compared with the first term (if there are not abrupt wind gusts), and since the first term can be approximated by the difference of vehicle velocities at two consecutive sampling time instants divided by the sample time interval, we can approximate $\Delta\hat{\mu}$ as

$$\Delta\hat{\mu} = \frac{1}{b1}\left[\dot{x}_1(t_k) - \dot{x}_1(t_{k-1}) \right] \tag{3.70}$$

We only require the sign of $\dfrac{\partial \mu}{\partial \lambda}$ instead of the exact value of $\dfrac{\partial \mu}{\partial \lambda}$. The sign of $\dfrac{\partial \mu}{\partial \lambda}$ can be calculated as

$$sgn\left(\frac{\partial \mu}{\partial \lambda} \right) = 1 \qquad\qquad if \quad \Delta\hat{\mu}\cdot\Delta\hat{\lambda} \geq 0$$

$$= -1 \qquad\qquad if \quad \Delta\hat{\mu}\cdot\Delta\hat{\lambda} < 0 \tag{3.71}$$

Target slip updating algorithm

The target slip is moved in the direction of the peak according to the sign of the slope of the $\mu - \lambda$ curve. The target is updated according to

$$\lambda_T(k+1) = \lambda_T(k) \pm sgn\left(\frac{\partial \mu}{\partial \lambda}\right) step(k) \qquad \text{+ for acceleration}$$

$$\qquad \qquad \qquad \qquad \qquad \text{- for deceleration} \qquad (3.72)$$

$$step(k+1) = 05 \cdot step(k) \qquad \text{if sign is changed}$$

$$step(k+1) = step(k) \qquad \text{if sign remains the same value}$$

$$step(0) = \alpha \qquad \text{initial value} \qquad (3.73)$$

where $\lambda_T(k)$ is the target slip at the time instant, k and α is an initial and a convenient value. For adapting at the varying road conditions, either the step size should have a lower bound or it should be re-initialized if the value of the estimated slope varies substantially after a steady value has been reached. Otherwise the speed of the estimation process would be substantially reduced because of too small a step size.

3.3.2.2 Fuzzy logic controller

The first two steps for minimum time control are the same as the sliding mode control case. The fuzzy logic slip control algorithm is used in step (3).

3.3.2.3 Simulation results (figure 3.12)

The controller must search for and maintain the peak slip value which gives the maximum tire traction force for the fastest acceleration. The peak slip value is 0.054 for the acceleration case and -0.11 for the deceleration case. Simulations are achieved for the ASMC, and the AFLC1. Each control method shows good performance in searching for and maintaining the peak slip value

3.3.3 Longitudinal platoon control

Longitudinal control strategies are necessary in order to regulate the spacing and velocity of vehicles in an automated highway system consisting of a platoon of vehicles. The controller must also insure good performance over a variety of operating points and external conditions without sacrificing safety or reliability.

Two-car and four-car computer simulations have demonstrated (Hedrick et al. 1990) the robustness of the developed longitudinal control algorithm. Two-car, three-car, and four-car longitudinal experiments have been conducted as part of the California PATH Program (Chang et al. 1992). These simulations and experiments, however, are performed without considering road condition

changes. They do not show the stability and the robustness when the road condition is widely varied. In fact, since the sliding mode controller is used in these works, the system may be unstable for icy road if the control gain is tuned for dry asphalt; and the control will be too conservative if the control gain is tuned for icy road.

The objective of this research is to show the possibility of using adaptive control algorithms to deal with the unknown time-varying road condition in the longitudinal platoon control. We will consider the two-car platoon in what follows.

3.3.3.1 Sliding mode controller

Figure 3.5 illustrates the spacing in a platoon with two vehicles.
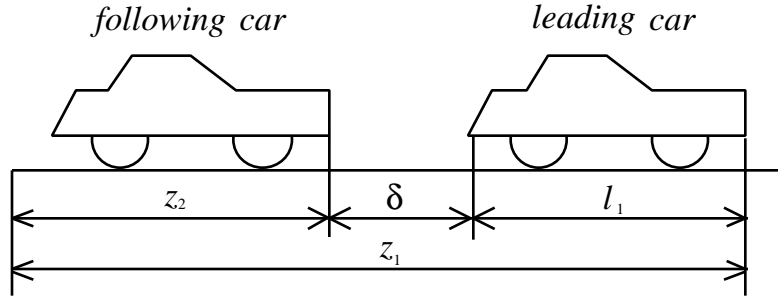
Figure 3.5 Platoon spacing

In the formulation of the longitudinal platoon control problem, we define a spacing error between two successive vehicles as :

$$\delta(t) = z_1(t) - z_2(t) - l_1 \tag{3.74}$$

where z indicates the position of the front of each vehicle and l_1 the length of the leading vehicle. Next, we define the spacing error as:

$$\varepsilon(t) = \delta_d(t) - \delta(t) \tag{3.75}$$

where δ_d is the desired spacing between two vehicles.

Since there is slip between the tire and the road surface, the states presented in section 3.1 have the following relationship:

$$x_2(t) = x_1(t) + r(t) \tag{3.76}$$

where $r(t) \neq 0$. Using this equation and equations (3.1) and (3.2), we can obtain the following equation:

$$\dot{x}_1(t) = \hat{f} + df + a_1 T + a_2 \dot{r}(t) \tag{3.77}$$

where $\hat{f} + df = -\dfrac{b_2 f_1 + b_1 f_2}{b_1 + b_2}$, $a_1 = \dfrac{b_1 b_3}{b_1 + b_2}$, and $a_2 = -\dfrac{b_1}{b_1 + b_2}$.

Since the control task of the platoon control is to track the velocity of the leading vehicle while maintaining a constant separation, an obvious choice for a sliding surface is one which incorporates the corresponding errors. Let the sliding surface be defined as

$$s = \dot{\varepsilon} + 2c_1 \varepsilon + c_1^2 \int_0^t \varepsilon \, dt = 0 \tag{3.78}$$

where ε is defined at equation (3.75). The coefficient c_1 is chosen to place the poles of the sliding surface. Differentiating the surface to obtain the input torque, T, yields:

$$\dot{s} = \ddot{\varepsilon} + 2c_1 \dot{\varepsilon} + c_1^2 \varepsilon \tag{3.79}$$

Substituting (3.77) into (3.79), and considering the sliding condition yields:

$$\dot{s} = R_w \left(\hat{f} + df + a_1 T + a_2 \dot{r} \right) - a_{lead} + 2c_1 \dot{\varepsilon} + c_1^2 \varepsilon = -Ksat\left(\frac{s_1}{\Phi}\right) \tag{3.80}$$

Because the value of $r(t)$ is unknown, it is difficult to obtain the input torque, T. To obtain some information about $r(t)$, a differential equation for $r(t)$ can be derived subtracting (3.1) from (3.2):

$$\dot{r} = (f_1 - f_2) - (b_1 + b_2)\mu(\lambda) + b_3 T \tag{3.81}$$

Considering this equation, we know that the maximum variation of $\dot{r}(t)$ is about $0.7T$ when road conditions are abruptly changed from dry asphalt to icy road. Since $a_1 \approx a_2$ in equation (3.80), this $\dot{r}(t)$ can not be ignored while the input torque T is constructed. If we assume no slip condition, i.e., $\dot{r}(t) = r(t) = 0$, then the system may be unstable (when deciding control gains by ignoring $\dot{r}(t)$) or have too conservative control (when including $\dot{r}(t)$ in df). Therefore, it is dangerous to ignore the slip when adverse road conditions are expected or hard maneuvers (rapid change of the input torque) are required.

Because of the difficulty caused by the unknown function $r(t)$, we use an alternate approach using two sliding surfaces proposed by Hedrick (Hedrick et

al. 1990). The first sliding surface is used to define a "synthetic (or fictitious) control". The synthetic control is then used to define the desired trajectories for the second sliding surface which, upon differentiation, yields the control variable. For our system, $\mu_{des}(\lambda_{des})$ will be the synthetic (or fictitious) control for the first sliding surface, and it is further controlled by the second sliding surface using the system control input T. If the desired trajectory of the second surface can be tracked within an acceptable bound, then the original trajectory can also be expected to track within an acceptable bound.

Utilizing this technique, a primary surface is defined the same as (3.67):

$$s_1 = \dot{\varepsilon} + 2c_1\varepsilon + c_1^{\,2}\int_0^t \varepsilon\,dt = 0 \tag{3.82}$$

Substituting (3.1) instead of (3.77) into (3.79) and considering the sliding condition yields:

$$\dot{s}_1 = -f_1 + b_1\mu(\lambda) - a_{lead} + 2c_1\dot{\varepsilon} + c_1^{\,2}\varepsilon = -\eta_1 sat\left(\frac{s_1}{\Phi}\right) \tag{3.83}$$

Then, the desired adhesive coefficient is

$$\mu_{des}(\lambda_{des}) = \frac{1}{b_1}\left[f_1 + a_{lead} - 2c_1\dot{\varepsilon} - c_1^{\,2}\varepsilon - \eta_1 sat\left(\frac{s_1}{\Phi}\right) \right] \tag{3.84}$$

The next step is calculating λ_{des} from μ_{des}. To accomplish this, equation (3.12) can be used. If we do not estimate the road condition [14], we should assume $a_t = rc$ at some nominal value, such as a middle value between 0.8 (dry asphalt) and 0.3 (icy road). However this will again result in system instability (when nominal value is high) or in conservative control (when nominal value is small). If road condition estimation, $\hat{a}_t(t)$, is available, equation (3.12) can be used to calculate λ_{des} from μ_{des} by assuming that $\hat{a}_t(t)$ approximates $a_t(t)$.

To achieve the desired slip, we control the wheel slip directly at the desired value using the same algorithm for slip control. By defining the second sliding surface as

$$s_2 = \lambda_e = 0 \tag{3.85}$$

we can obtain the desired torque T_{des}. (see section 3.3.1.1)

3.3.3.2 Fuzzy logic controller

As with the sliding mode platoon controller, the fuzzy logic platoon controller consists of two consecutive steps. Both use adaptive fuzzy logic control algorithms which have different fuzzy variables and outputs. In the first step, ε and $\dot{\varepsilon}$ are chosen as the fuzzy variables to infer a fictitious control input λ_{des}. It should be noticed that equation (3.12) is not necessary to calculate λ_{des} from μ_{des} since λ_{des} can be directly achieved in the first step of fuzzy logic control. Twenty five fuzzy control rules are chosen based on engineering judgment (table 3), and they are used for the initial rules of the adaptive fuzzy control algorithm.

Table 3 Fuzzy rule tables for λ_{des}

		ε				
		NB	NS	ZO	PS	PB
$\dot{\varepsilon}$	NB	PB	PB	PB	NS	NS
	NS	PB	PB	PS	NS	NB
	ZO	PB	PS	ZO	NS	NB
	PS	PB	PS	NS	NB	NB
	PB	PS	PS	NB	NB	NB

To achieve the desired slip, we use the adaptive fuzzy logic slip controller which is already derived in section 3.3.1.2.

3.3.3.3 simulation results (figure 3.13)

The objective of the longitudinal platoon control is to regulate the spacing error among the vehicles in a platoon. As mentioned before, simulations are achieved for a two car platoon (lead car and one car following).

Figure 3.13 shows the results of the adaptive fuzzy control and the sliding mode control with road condition estimation, respectively, with system uncertainties. Because of the system uncertainties, each controller cannot track the desired friction coefficient accurately and, thus, spacing errors occur. In this case, the adaptive fuzzy control shows better performance (less spacing error) than the sliding mode controller.
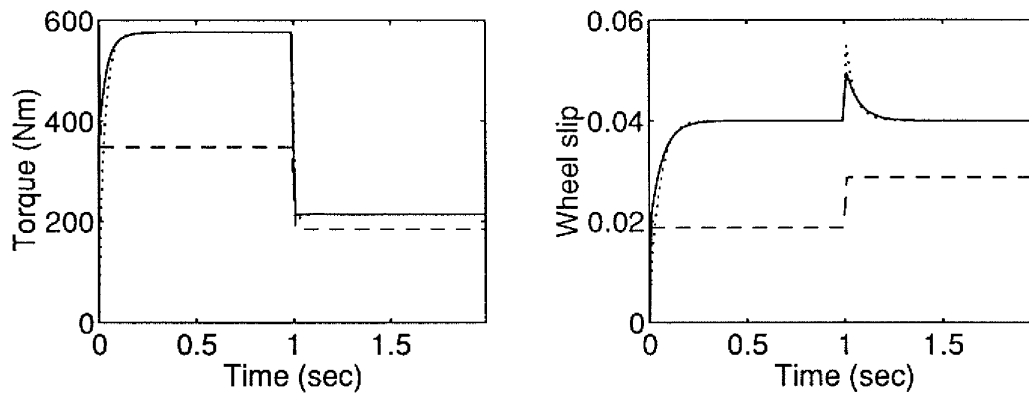
(a) Acceleration (Desire slip = +0.04)
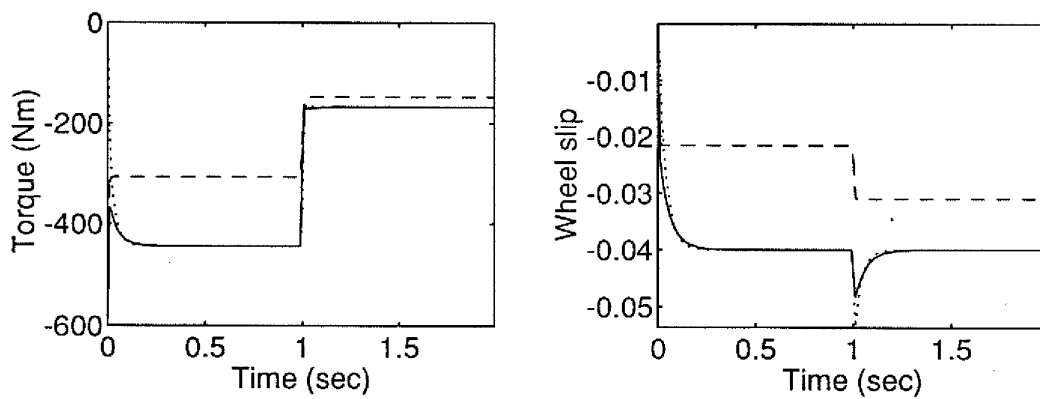
(b) Deceleration (Desire slip = -0.04)

Figure 3.6 Slip control - SFLC and AFLC
Abrupt road condition change (Dry asphalt → Icy road)
———————— : SFLC   ················ : AFLC0   ——————— : AFLC1
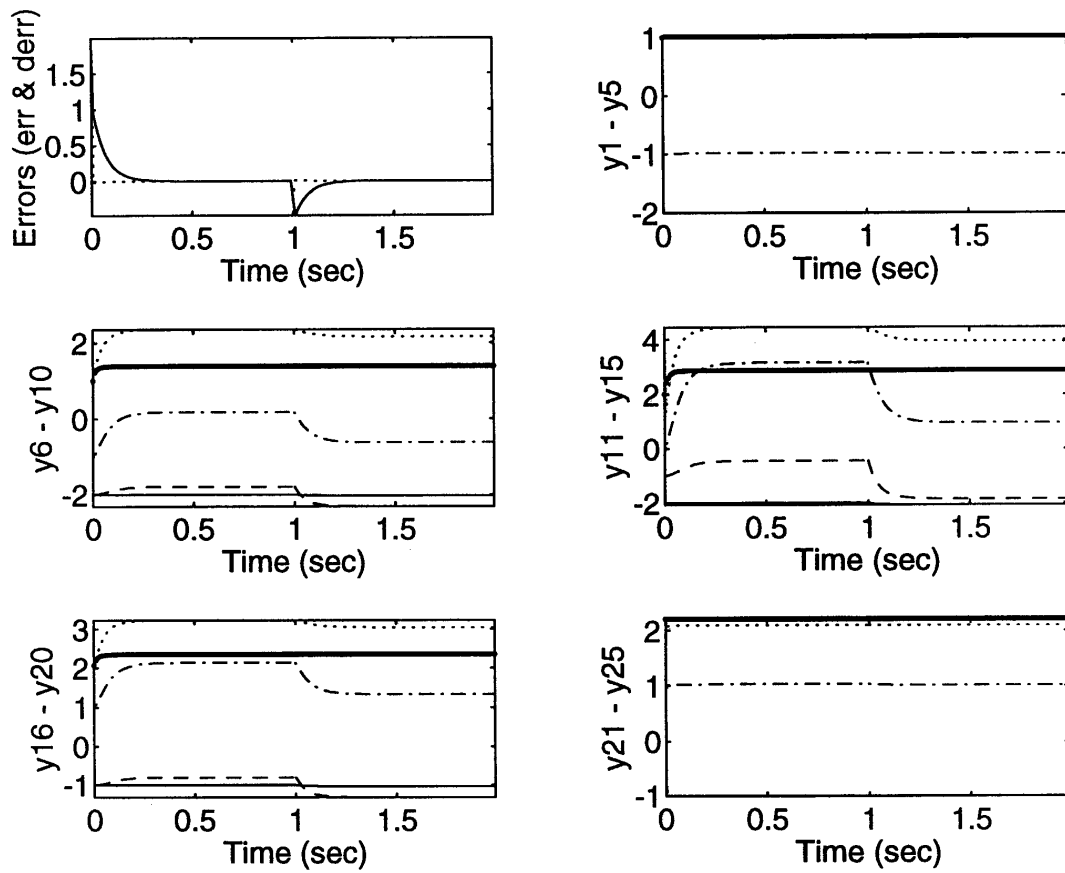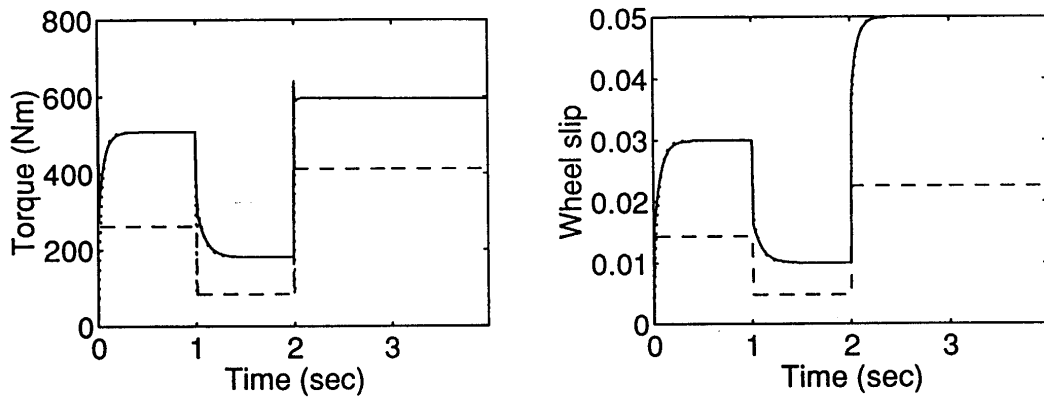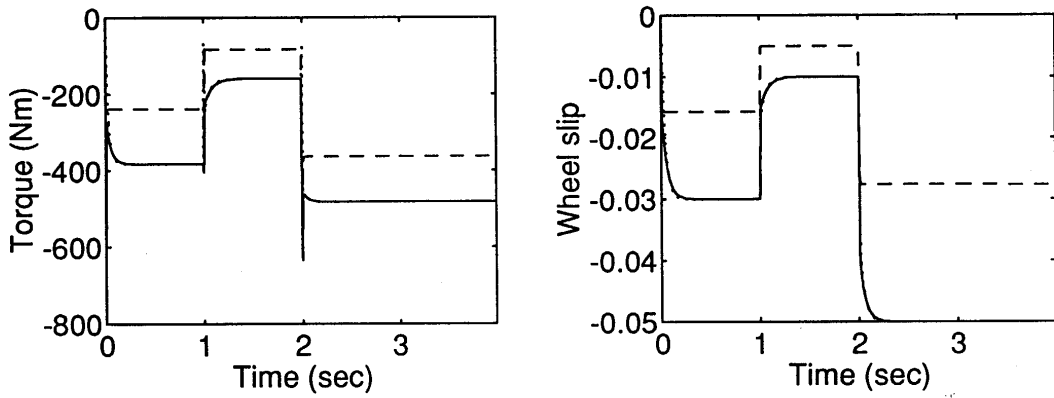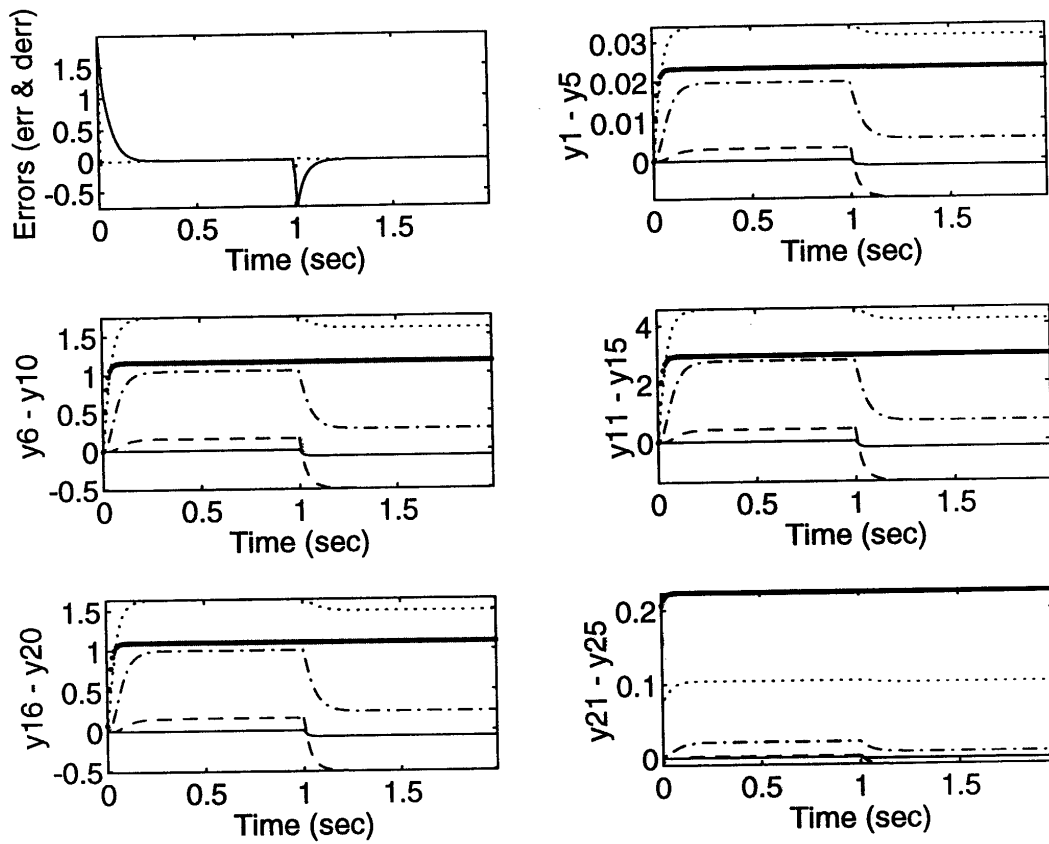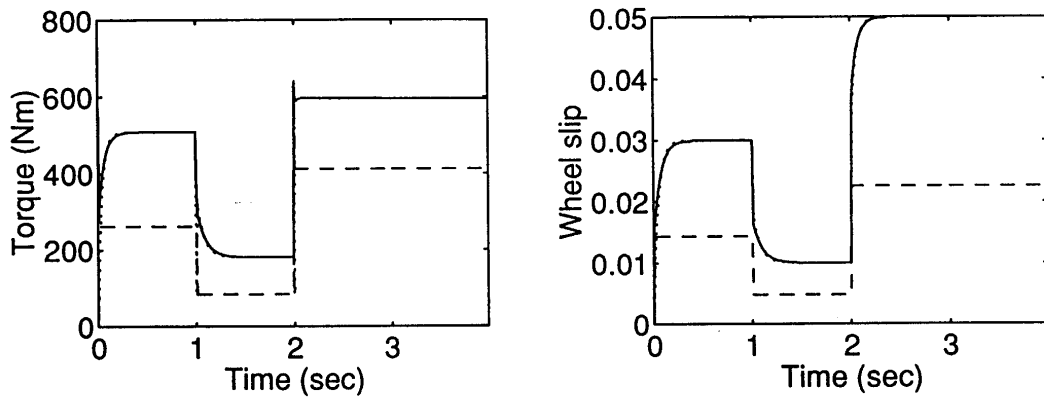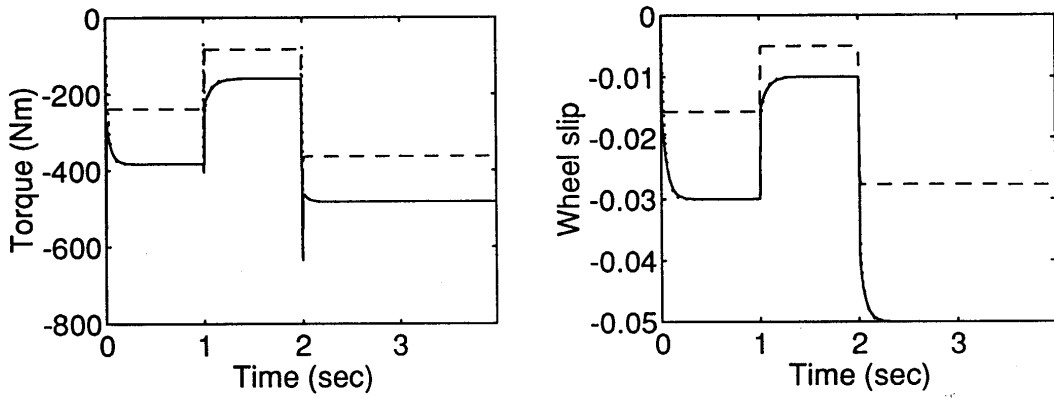
Figure 3.7 Controller parameters of AFLC1
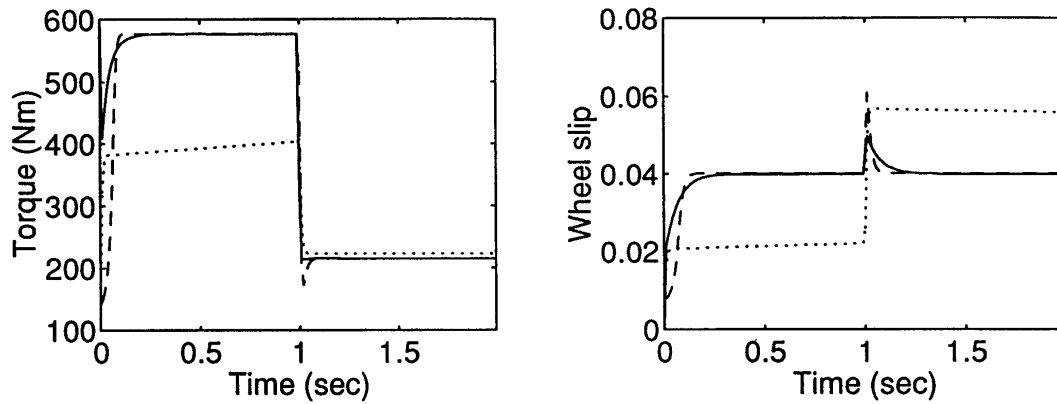
(a) Acceleration (Desire slip = +0.03, +0.01, +0.05)

(b) Deceleration (Desire slip = -0.03, -0.01, -0.05)

Figure 3.9 Slip control - SFLC and AFLC
Dry asphalt

------------ : SFLC   ··············· : AFLC0 ——————— : AFLC1

Figure 3.8 Controller parameters of AFLC0

(a) Acceleration (Desire slip = +0.03, +0.01, +0.05)
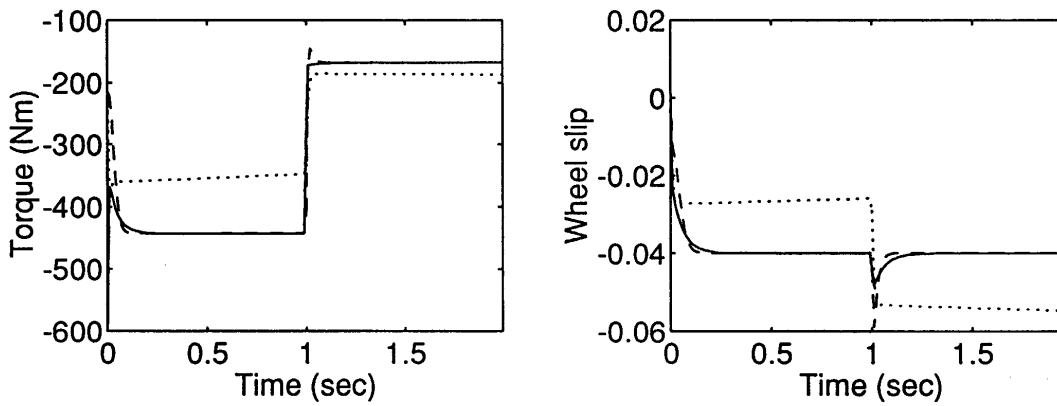

(b) Deceleration (Desire slip = -0.03, -0.01, -0.05)

Figure 3.9 Slip control - SFLC and AFLC
Dry asphalt

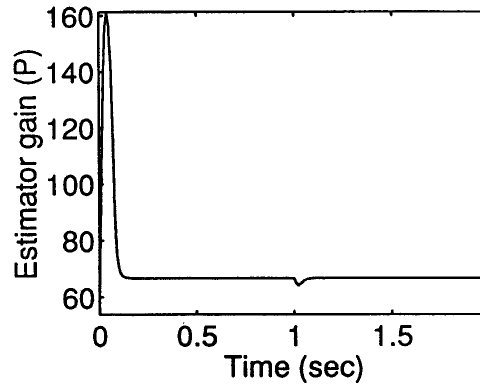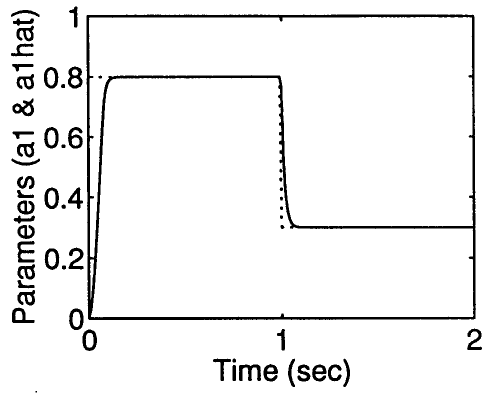------------ : SFLC   ················ : AFLC0   ———————— : AFLC1
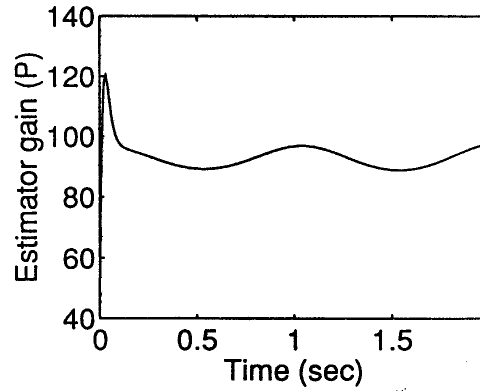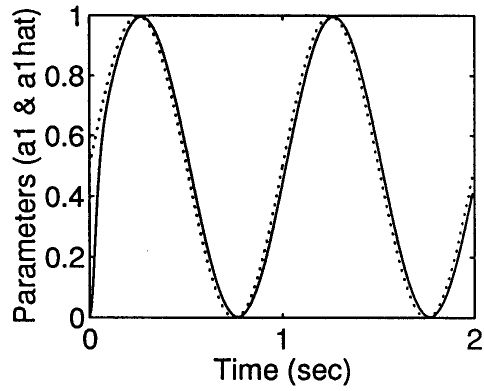
(a) Acceleration (Desire slip = +0.04)

(b) Deceleration (Desire slip = -0.04)

Figure 3.10 Slip control - AFLC and SMC
Abrupt road condition change (Dry asphalt → Icy road)
————— : AFLC1   ------------ : ASMC   ·············· : SSMC

(a) Abrupt road condition change (Dry asphalt → Icy road)

(b) Sinusoidal road condition change

Figure 3.11 On-line road condition estimation
Including disturbance or measurement noise (5*sin(60t))
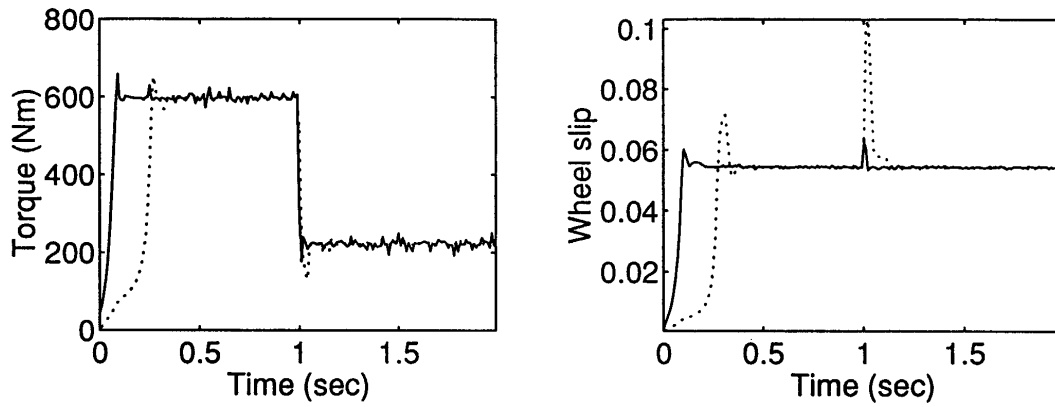
(a) Acceleration

(b) Deceleration

Figure 3.12 Fastest acceleration and deceleration control
Abrupt road condition change (Dry asphalt → Icy road)
———————— : AFLC1   ·············· : ASMC

Figure 3.13 Longitudinal platoon control

————— : AFLC1   ················ : ASMC

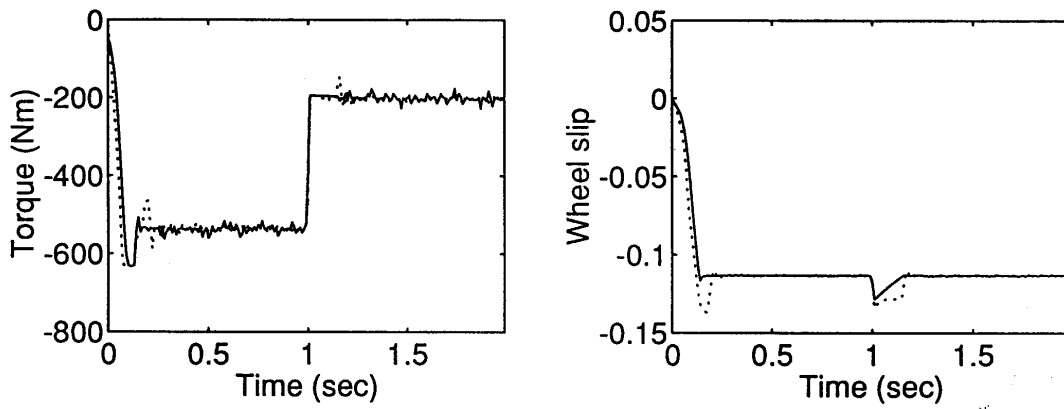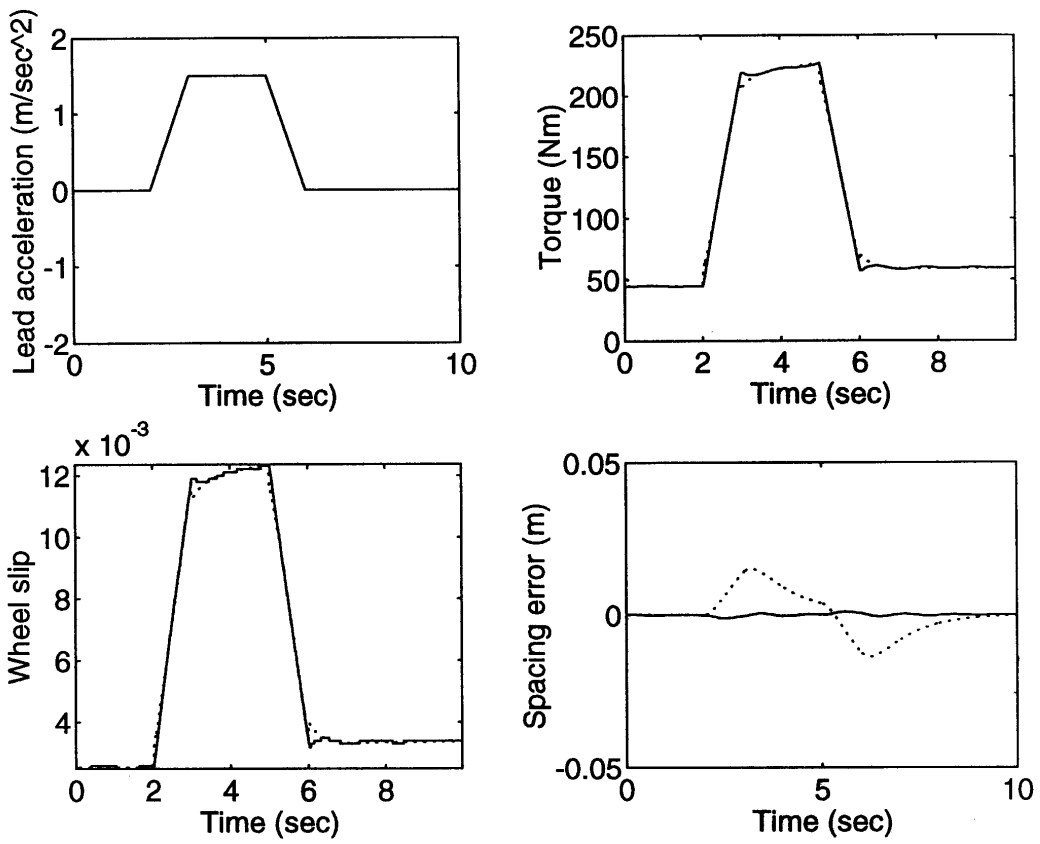## 4. Complex vehicle model

In this section, a complex vehicle model is described and a simplified vehicle model is derived for analysis and controller design. The adaptive sliding mode controller and adaptive fuzzy logic controller are designed based on the simplified model and they are evaluated by simulations using the complex model.

4.1 system description

4.1.1 Vehicle model

The complex vehicle model is utilized to simulation the dynamic behavior of the vehicle as realistically as possible. It consists of

i) Ford engine model
ii) torque converter model (McMahon et al. 1991)
iii) the COMPLEX dynamic model (Peng 1992)

It includes six degree of freedom for the vehicle sprung mass, four wheel states, two engine states, and a torque converter model. Additionally, the brakes, throttle, and steering actuators are modeled as linear first order systems. The inputs to the front-wheel driven and front-wheel steered model are the steering angle, throttle angle, and brake pressure. So, the vehicle is described by the following 18 states:

$$\left(x, v_x, y, v_y, z, v_z, \theta, \dot{\theta}, \phi, \dot{\phi}, \psi, \dot{\psi}, m_{air}, \omega_{eng}, \omega_w, T_{brake}, \alpha, \delta\right)$$

The inputs are $\left(T_{brk_{com}}, \alpha_{com}, \delta_{f_{com}}\right)$ and the outputs are $(\lambda, \varepsilon, y_s)$. The model does not include any transmission dynamics or engine delays. The resulting equations for the complex vehicle model are shown in appendix D.

Specifically, all engine and torque converter parameters are obtained from the Ford Lincoln Towncar, while all chassis, suspension and tire characteristics are obtained from the Toyota Celica. It implies that the simulation results may not be very realistic quantitatively. However, it is expected that the qualitative performance should still be similar to actual test vehicles.

It should be noted that, while every desired torque in the simple model is assumed to be attainable, the complex model has a saturation for the total torque because of the saturation of the engine throttle or braking torque. Therefore, it is important to keep this restriction in mind during design of the controller or tuning control gains. Unlike the simple vehicle model, the complex vehicle model has two tires (front and rear) as the controlled outputs even after

assuming a bicycle model. In this report, it is assumed that only one control input is available (total torque which is the difference between engine torque and the brake torque). To deal with this constraint, we properly derived the controller equations so that every control objective can be achieved by controlling only the front wheel slip.

4.1.2 Simplified vehicle model

The complex vehicle model for the simulation, which fully describes the dynamic behavior of the vehicle, is too complex for analysis and controller design. Therefore, it is necessary to make assumptions which will reduce the model to a simplified form, yet still capture the fundamental plant behavior. The complex vehicle model is simplified by

(i) neglecting the roll, pitch, and vertical motion.
(ii) assuming bicycle model (i.e. the dynamics of the left and right side of the vehicle are identical)
(iii) discounting the actuator and manifold dynamics
(iv) locking the torque converter (i.e. $\omega_{eng} \approx \dfrac{\omega_w}{r^*}$, $T_{pump} \approx r^* T_{shaft}$, $r^* = r_{drive} r_{gear}$)

Simulations have revealed that the first simplification (i) is valid without any appreciable loss in accuracy under typical to slightly severe environmental conditions. If there are no severe steering maneuvers, simplification (ii) is also generally valid. The last simplification (iv) requires the vehicle to operate under conditions of low torque transfer between the engine and the turbine ($\omega_{turb} / \omega_{eng} \approx 1$). This requirement is not uniformly met, especially during moderate to heavy braking or immediately after a gear shift. Unlike the general no slip assumption, the tire slip is considered in this work ($r_{wf} \omega_{wf} \neq v$) for traction control and, unlike other simple vehicle model, the angular velocities of the front and rear tire have different values ($\omega_{wf} \neq \omega_{wr}$).

The resulting equations of the simplified vehicle model are

$$\dot{v}_x = ff_1 + \frac{1}{m} F_{x\,tot} \tag{4.1}$$

$$ff_1 = -\frac{1}{m} \left[c_x v_x^2 + F_{roll} - m v_y \dot{\psi} \right] \tag{4.2}$$

$$F_{x\,tot} = 2 \left(F_{xf} + F_{xr} \right) \tag{4.3}$$

$$\dot{\omega}_{wf} = \frac{1}{J_{wf}} \left[0.5 T_{shaft} - 0.3 T_{brake} - r_{wf} F_{xf} \right] \tag{4.4}$$

If torque converter is locked,

$$T_{shaft} = \frac{1}{r^*}\left[T_{net} - J_{eng}\frac{\dot{\omega}_{wf}}{r^*}\right]$$ (4.5)

Then, (4.4) can be written as

$$\dot{\omega}_{wf} = \frac{r^*}{J^*}\left[T_{tot} - r^*r_{wf}F_{xf}\right]$$ (4.6)

$$J^* = 2J_{wf}r^{*2} + J_{eng}$$ (4.7)

$$T_{tot} = T_{net} - 0.6r^*T_{brake}$$ (4.8)

4.1.3 Wheel slip dynamic equation

Acceleration case

During acceleration, front wheel slip can be written as

$$\lambda_f = \frac{\omega_{wf}r_{wf} - v}{\omega_{wf}r_{wf}} = \frac{x_2 - x_1}{x_2}$$ (4.9)

By differentiating this equation, we obtain

$$\dot{\lambda}_f = \frac{\partial\lambda_f}{\partial x_1}\frac{\partial x_1}{\partial t} + \frac{\partial\lambda_f}{\partial x_2}\frac{\partial x_2}{\partial t}$$

$$= \frac{1}{\omega_{wf}r_{wf}}\left[(1-\lambda_f)r_{wf}\frac{r^*}{J^*}\left\{T_{tot} - r^*r_{wf}F_{xf}\right\} - \left(ff_1 + \frac{1}{m}F_{x\,tot}\right)\right]$$ (4.10)

Deceleration case

Using the same method as the acceleration case, we obtain

$$\lambda_f = \frac{\omega_{wf}r_{wf} - v}{v} = \frac{x_2 - x_1}{x_1}$$ (4.11)

$$\dot{\lambda}_f = \frac{1}{v}\left[r_{wf}\frac{r^*}{J^*}\left\{T_{tot} - r^*r_{wf}F_{xf}\right\} - (1+\lambda_f)\left(ff_1 + \frac{1}{m}F_{x\,tot}\right)\right]$$ (4.12)

4.1.4 Tire equation and road condition estimation algorithm

We use the same tire model and the on-line road condition estimation scheme as that for the simple vehicle model derived in section 3.2.1.2.

4.2 Controller design and application

Since every method for designing controllers in this section is the same as the previous section (section 3). we will give just a short explanation.

4.2.1 Slip control

4.2.1.1 Sliding mode controller

The first switching surface is defined as

$$s_1 = \lambda_e + c_1 \int_0^t \lambda_e \, dt = 0 \tag{4.13}$$

where $\lambda_e = \lambda_f - \lambda_{f\,des}$, and $\lambda_{f\,des}$ is the desired front wheel slip. In order to obtain the vehicle controls, we differentiate this surface:

$$\dot{s}_1 = \dot{\lambda}_f - \dot{\lambda}_{f\,des} + c_1 \lambda_e \tag{4.14}$$

Substituting in the slip dynamic equation (4.10, 4.12) and inserting sliding condition yields the following control law for the desired total torque input to the drive wheel.

Acceleration case

$$T_{tot\,des} = \frac{\omega_{wf} r_{wf}}{aa_1} \left[\frac{aa_1}{\omega_{wf} r_{wf}} r^* r_{wf} F_{xf} + \frac{1}{\omega_{wf} r_{wf}} \left(ff_1 + \frac{1}{m} F_{x\,tot} \right) + \dot{\lambda}_{f\,des} - c_1 \lambda_e - \eta \, sat\left(\frac{s_1}{\Phi_1} \right) \right] \tag{4.15}$$

$$aa_1 = \left(1 - \lambda_f \right) r_{wf} \frac{r^*}{J^*} \tag{4.16}$$

Deceleration case

$$T_{tot\,des} = \frac{v}{bb_1} \left[\frac{bb_1}{v} r^* r_{wf} F_{xf} + \frac{1 + \lambda_f}{v} \left(ff_1 + \frac{1}{m} F_{x\,tot} \right) + \dot{\lambda}_{f\,des} - c_1 \lambda_e - \eta \, sat\left(\frac{s_1}{\Phi_1} \right) \right] \tag{4.17}$$

$$bb_1 = r_{wf} \frac{r^*}{J^*} \tag{4.18}$$

The desired engine or brake torque is found from $T_{tot\,des}$. A protocol is set up to choose between either the brake or throttle input (Pham 1992). The logic flow is illustrated in figure 4.1. The 60/40 division of T_{brake} is applied to determine the desired brake torque for the front wheel.
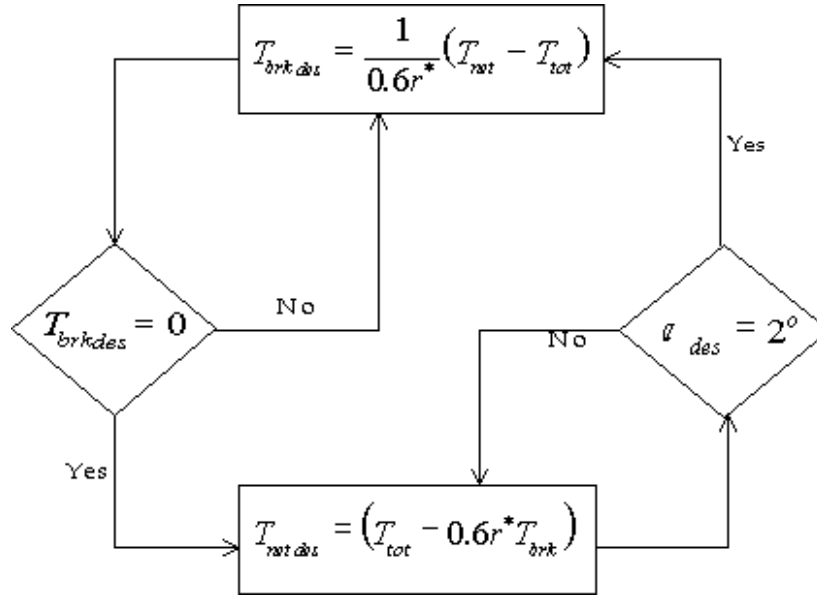
$$T_{brk\,des} = \frac{1}{0.6r^*}\left(T_{net} - T_{tot}\right)$$

$$T_{brk\,des} = 0$$

$$\alpha_{des} = 2^o$$

$$T_{net\,des} = \left(T_{tot} - 0.6r^* T_{brk}\right)$$

Figure 4.1 Brake/Throttle decision flowchart

To track the input torque, $T_{tot\,des}$, we need to define separate surfaces for the throttle and brake inputs. Recall that the input torque is equal to the sum of the engine torque and brake torque. Thus, to track the desired brake torque, we define:

$$s_2 = T_{brk} - T_{brk\,des} = 0 \tag{4.19}$$

It is less straight-forward to track the desired engine torque because there is no direct relation between the throttle and $T_{net\,des}$. However, the torque quantity can be translated into an equivalent desired pressure, $P_{man\,des}$ (or, assuming ideal gas behavior, $m_{air\,des}$). Then, the desired throttle angle, α_{des}, can be uniquely obtained for a given engine speed. To track the desired manifold trajectory, we define:

$$s_3 = m_{air} - m_{air\,des} = 0 \tag{4.20}$$

Differentiating the secondary surface yields:

$$\dot{s}_2 = \dot{T}_{brk} - \dot{T}_{brk\,des}$$
$$= \frac{1}{\tau_{brk}}\left(T_{brk\,com} - T_{brk}\right) - \dot{T}_{brk\,des} \tag{4.21}$$

$$\dot{s}_3 = \dot{m}_{air} - \dot{m}_{air\,des}$$
$$= MAX * PRI(P_{man}) * TC(\alpha) - \dot{m}_{air\,out} - \dot{m}_{air\,des} \tag{4.22}$$

By substituting sliding mode, the command inputs are found to be:

$$T_{brk\,com} = \tau_{brk}\left[\frac{1}{\tau_{brk}}T_{brk} + \dot{T}_{brk\,des} - \eta_2 sat\left(\frac{s_2}{\Phi_2}\right)\right] \qquad (4.23)$$

$$TC(\alpha) = \frac{1}{MAX * PRI(P_{man})}\left[\dot{m}_{air\,out} + \dot{m}_{air\,des} - \eta_3 sat\left(\frac{s_3}{\Phi_3}\right)\right] \qquad (4.24)$$

where the control gains, η_i's, are selected so that the suitable conditions are satisfied. Typically, the secondary surface gains are selected to be much larger than the gains of the primary surface.

4.2.1.2 Fuzzy logic controller

To obtain $T_{tot\,des}$, the same method as section 3.3.1.2. is used. In this case, the fuzzy variables are λ_e and $\dot{\lambda}_e$, and λ_e is defined as

$$\lambda_e = \lambda_f - \lambda_{f\,des} \qquad (4.25)$$

4.2.1.3 Simulation results (figure 4.2)

Figure 4.2 shows the simulation results of slip control for the front wheel when the desired front wheel slip is abruptly changed. Each controller shows good performance for the different road conditions. The fluctuation, which is shown near the start part of the adaptive fuzzy logic control case, may occur because of the poor choice of the initial rules. The fluctuation is reduced as the controller parameter values ($\bar{u}_c^i$) are adapted enough.

4.2.2 Minimum time control (minimum time acceleration or deceleration)

The control algorithm of sliding mode control with road condition estimation and adaptive fuzzy logic control for minimum time control is the same as the simple model case derived in section 3.3.2. The simulation results are shown in figure 4.3.

4.2.3 Longitudinal platoon control

Because of the same reason described in section 3.3.3.1, we use two sliding surfaces approach. Let the first sliding surface be defined as

$$s_1 = \dot{\varepsilon} + 2c_1\varepsilon + c_1^2\int_0^t \varepsilon dt = 0 \qquad (4.26)$$

where $\varepsilon = x - x_{lead}$ is the spacing error. For the first sliding surface, $F_{xtot\,des}\left(\lambda_{f,r\,des}\right)$ is the control input, which is further controlled by the second sliding surface using the system control input torque T. In order to obtain the desired traction force, we differentiate this surface:

$$\dot{s}_1 = \ddot{\varepsilon} + 2c_1\dot{\varepsilon} + c_1^2\varepsilon$$

$$= ff_1 + \frac{1}{m}F_{xtot} - a_{lead} + 2c_1\dot{\varepsilon} + c_1^2\varepsilon \qquad (4.27)$$

where $\ddot{\varepsilon} = \dot{v}_x - a_{lead}$. If considering the sliding condition, the total desired traction force is:

$$F_{x\,totdes} = -m\left[ff_1 - a_{lead} + 2c_1\dot{\varepsilon} + c_1^2\varepsilon + \eta_1 s_1\right] \qquad (4.28)$$

Then, by using the road condition estimation, the desired front wheel slip can be determined from this total desired traction force. This desired slip can be achieved by the slip control.

4.2.3.1 Simulation result (figures 4.4 and 4.5)

The simulations are performed to show the effect of traction control on the longitudinal platoon control. These are compared with the non-traction control case in which no slip is assumed. Sliding mode controller is used for each control.

Figure 4.4 shows the results of platoon control for the dry asphalt road condition and a mild accelerating maneuver. The spacing error can be reduce by traction control as shown in these figures. The significant advantage of the traction control occurs when driving condition is adverse. figure 4.5 shows the results of platoon control for poor road conditions and severe acceleration maneuvers. As shown in this figure, severe tire spinning occurs during acceleration when the non-traction control is used. If wheel slip exceeds the peak value (about 0.064), tire spinning occurs. In this case, the traction controller prevents this tire spinning and, at the same time, reduces the spacing error. Furthermore, it makes steering possible during this severe driving condition because it maintains the wheel slip in the positive slope (stable) region.
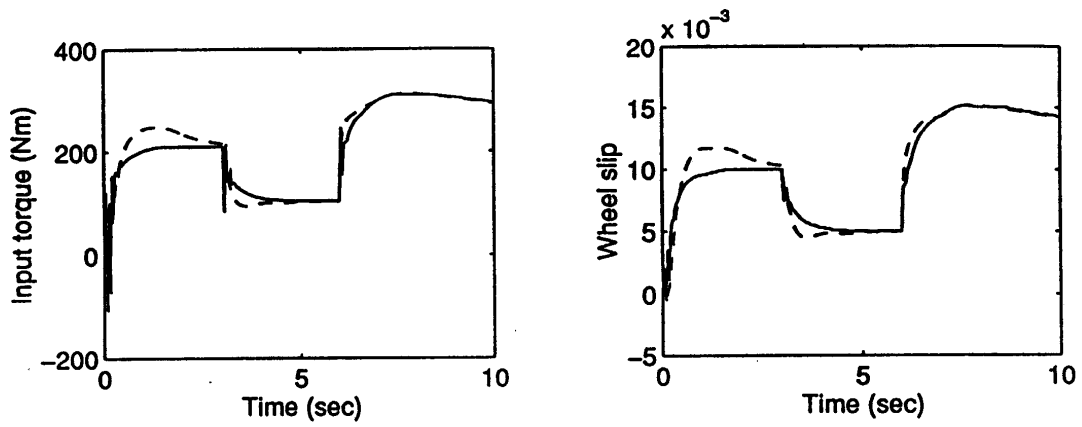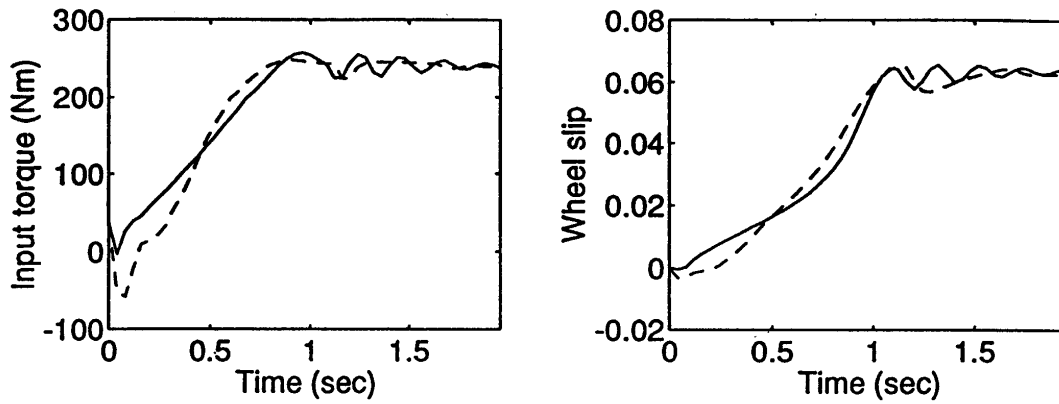
(a) Dry asphalt
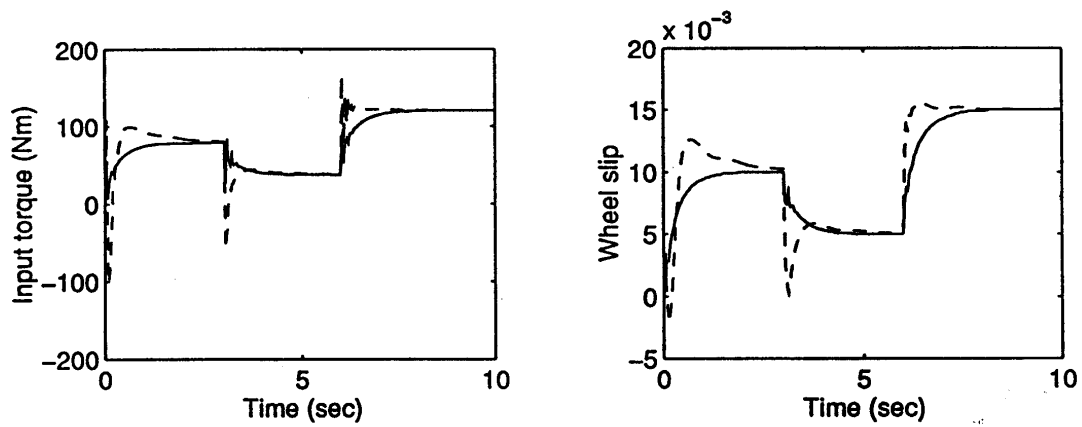
(b) Icy road

Figure 4.2 Slip control - AFLC and ASMC
Acceleration-desired slip = +0.01, +0.005, and +0.015
———— : AFLC ------------- : ASMC

(a) Acceleration (Target slip = +0.064)
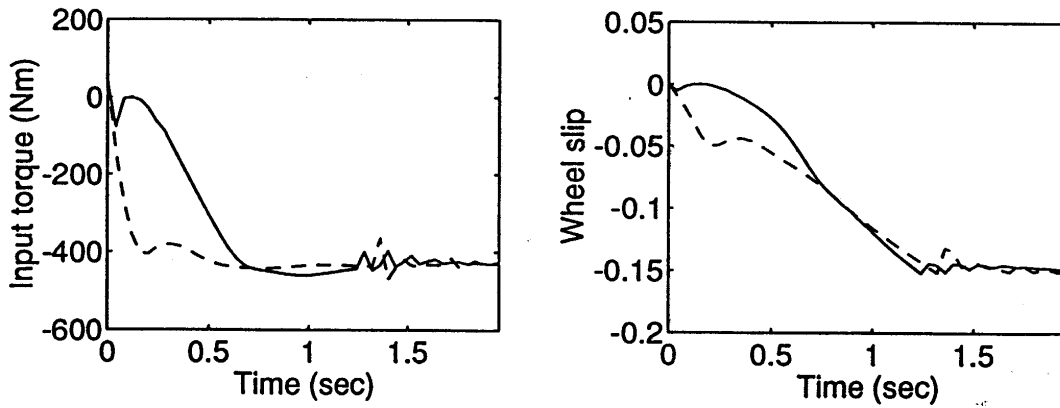
(b) Deceleration (Target slip = -0.13)

Figure 4.3 Fastest acceleration and deceleration control
Abrupt road condition change (Dry asphalt → Icy road)
————— : AFLC   ------------ : ASMC

Figure 4.4 Longitudinal platoon control
Dry asphalt and acceleration increment = 0.3
————— : Traction control   ------------- : Without traction control

Figure 4.5 Longitudinal platoon control
Icy road and acceleration increment = 0.45
————— : Traction control   ------------- : Without traction control
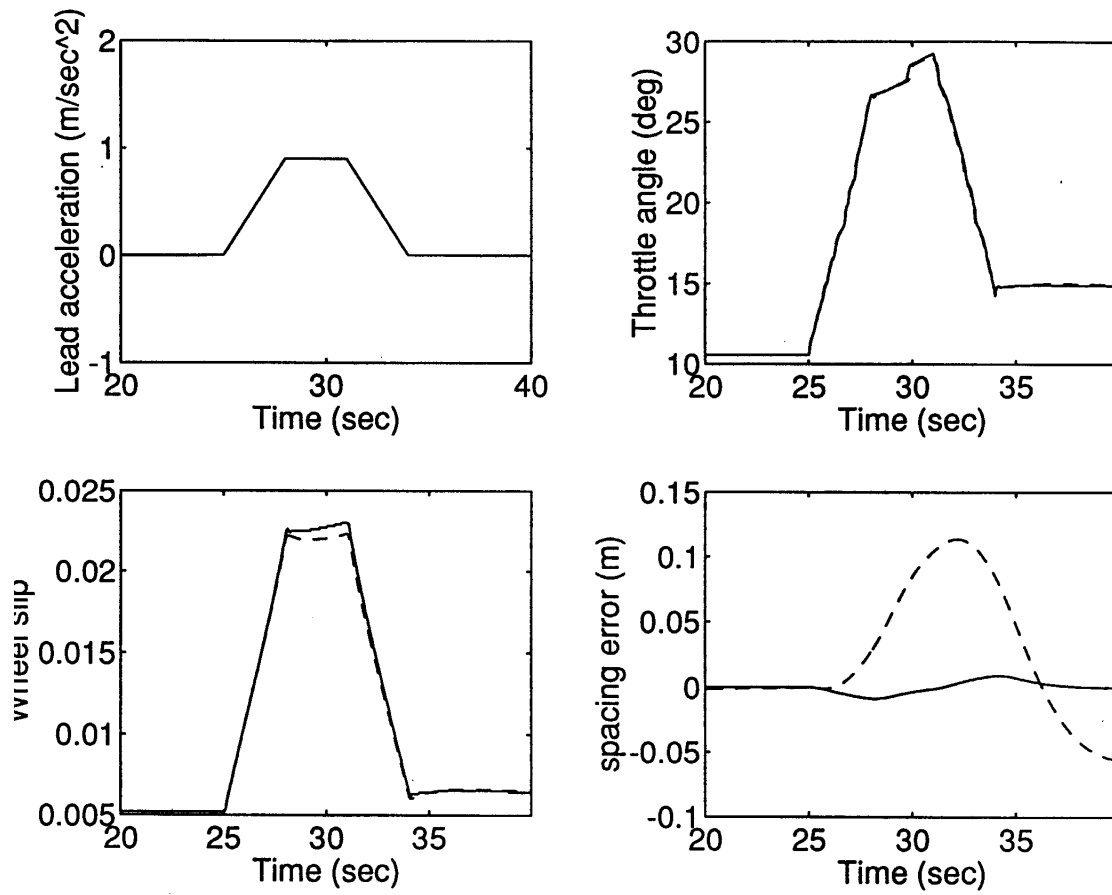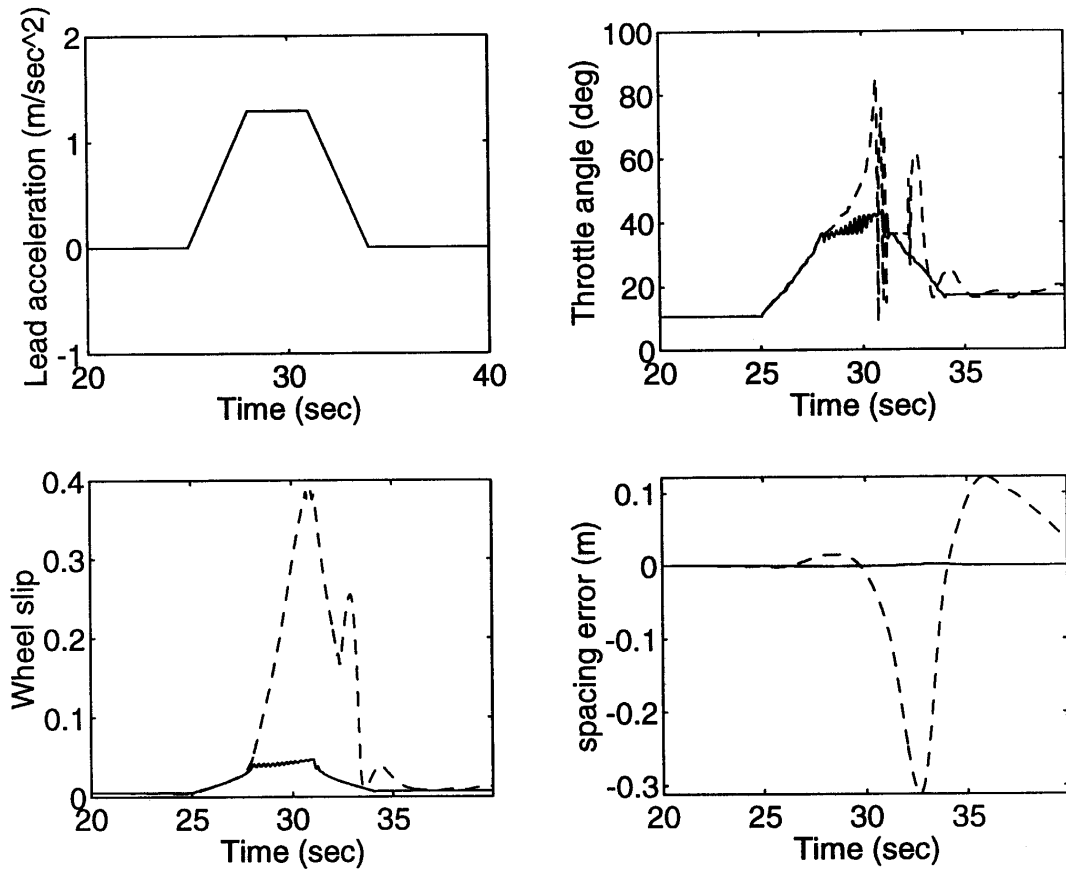
5. Conclusion and future study

1. This work has shown the importance of traction control for longitudinal control of vehicles in automation systems. Two control strategies, fuzzy logic control and sliding mode control, were studied for slip control, which in turn controls the traction. These controllers were designed and applied for the simple vehicle model and the complex vehicle model. It was shown how these traction control algorithms can be used to satisfy different objectives of vehicle traction control.

2. Adaptive algorithms were introduced to each of the sliding mode and fuzzy logic control methods to deal with unknown interaction between the tires and the road surface. The resulting control algorithms were sliding mode control with on-line road condition estimation and stable adaptive fuzzy logic control. These adaptive control algorithms give more stable and robust performance than standard sliding mode and fuzzy logic control algorithms, which do not have any adaptive algorithm.

3. Each of the adaptive traction controllers can be used to enhance the performance of a single independent vehicle, or a platoon of vehicles. It can be used to accelerate or decelerate a single vehicle in the minimum time, or it can be used to prevent the wheel from spinning or skidding. On the other hand, traction control improves the performance of two car platoon in terms of stability and achieves a tighter control. Traction control makes the system robust to external disturbances and parameter uncertainty.

4. The comparative study between adaptive sliding mode control and adaptive fuzzy logic control shows that each control method has its own advantages and disadvantages depending on the objectives considered. We have not yet reached a definite conclusion on which controller is better even if the road condition estimation scheme in adaptive sliding model control has some restriction. For this conclusion, in particular, experimental work is required to support any conclusion.

Appendix A. Proof of the Universal Approximation Theorem

We use the following Stone-Weierstrass Theorem to prove the Universal Approximation Theorem.

Stone-Weierstrass Theorem **:** [Rudin 1976, 28]
Let Z be a set of real continuous functions on a compact set U. If:
(i) Z is an *algebra*, that is, the set Z is closed under addition, multiplication, and scalar multiplication;
(ii) Z *separates points on* U, that is, for every $\mathbf{x}, \mathbf{y} \in U$, $\mathbf{x} \neq \mathbf{y}$, there exists $f \in Z$ such that $f(\mathbf{x}) \neq f(\mathbf{y})$; and
(iii) Z *vanishes at no point of* U, that is, for each $\mathbf{x} \in U$ there exists $f \in Z$ such that $f(\mathbf{x}) \neq 0$;
then the uniform closure of Z consists of all real continuous functions on U, that is, (Z, d_∞) is dense in $(C[U], d_\infty)$.

Let Y be the set of all fuzzy logic systems in the form of (3.35). In order to use the Stone-Weierstrass Theorem to prove the Universal Approximation Theorem, we need to show that Y is an algebra, Y separates points on U, and Y vanishes at no point of U. The following Lemmas A.1-A.3 prove that Y has these properties.

Lemma A.1: (Y, d_∞) is an algebra.

Proof: Let $f_1, f_2 \in Y$, so that we can write them as

$$f_1(\mathbf{x}) = \frac{\sum_{j=1}^{k_1} \bar{z}_1^{\,j} \left(\prod_{i=1}^{n} \mu_{A 1_i^j}(x_i) \right)}{\sum_{j=1}^{k_1} \left(\prod_{i=1}^{n} \mu_{A 1_i^j}(x_i) \right)} \tag{a1}$$

$$f_2(\mathbf{x}) = \frac{\sum_{j=1}^{k_2} \bar{z}_2^{\,j} \left(\prod_{i=1}^{n} \mu_{A 2_i^j}(x_i) \right)}{\sum_{j=1}^{k_2} \left(\prod_{i=1}^{n} \mu_{A 2_i^j}(x_i) \right)} \tag{a2}$$

Hence,

$$f_1(\mathbf{x}) + f_2(\mathbf{x}) = \frac{\sum_{j_1=1}^{k_1} \sum_{j_2=1}^{k_2} \left(\bar{z}_1^{\,j_1} + \bar{z}_2^{\,j_2} \right) \left(\prod_{i=1}^{n} \mu_{A 1_i^{j_1}}(x_i) \mu_{A 2_i^{j_2}}(x_i) \right)}{\sum_{j_1=1}^{k_1} \sum_{j_2=1}^{k_2} \left(\prod_{i=1}^{n} \mu_{A 1_i^{j_1}}(x_i) \mu_{A 2_i^{j_2}}(x_i) \right)} \tag{a3}$$

Since $\mu_{A1_i^{j_1}}$ and $\mu_{A2_i^{j_2}}$ are Gaussian in form, their product $\mu_{A1_i^{j_1}}\mu_{A2_i^{j_2}}$ is also Gaussian in form (this can be verified by straightforward algebraic operations). Hence, (a3) is the same form as (3.35), so that $f_1 + f_2 \in Y$. Similarly,

$$f_1(\mathbf{x})f_2(\mathbf{x}) = \frac{\sum_{j_1=1}^{k_1}\sum_{j_2=1}^{k_2}\left(\bar{z}_1^{\,j_1}\bar{z}_2^{\,j_2}\right)\left(\prod_{i=1}^{n}\mu_{A1_i^{j_1}}(x_i)\mu_{A2_i^{j_2}}(x_i)\right)}{\sum_{j_1=1}^{k_1}\sum_{j_2=1}^{k_2}\left(\prod_{i=1}^{n}\mu_{A1_i^{j_1}}(x_i)\mu_{A2_i^{j_2}}(x_i)\right)} \tag{a4}$$

which is also in the same form of (3.35). Hence, $f_1f_2 \in Y$. Finally, for arbitrary $c \in R$,

$$cf_1(\mathbf{x}) = \frac{\sum_{j=1}^{k_1}c\bar{z}_1^{\,j}\left(\prod_{i=1}^{n}\mu_{A1_i^{j}}(x_i)\right)}{\sum_{j=1}^{k_1}\left(\prod_{i=1}^{n}\mu_{A1_i^{j}}(x_i)\right)} \tag{a5}$$

which is again in the form of (3.35). Hence, $cf_1 \in Y$.   Q.E.D.

Lemma A.2: (Y, d_∞) separates points on U.

Proof: We prove this by constructing a required f. That is, we specify the number of fuzzy sets defined in U and R, the parameters of the Gaussian membership functions, the number of fuzzy rules, and the statements of fuzzy rules, such that the resulting f (in the form of (3.35)) has the property that $f(\mathbf{x}^0) \neq f(\mathbf{y}^0)$ for arbitrarily given $\mathbf{x}^0, \mathbf{y}^0 \in U$ with $\mathbf{x}^0 \neq \mathbf{y}^0$. Let $\mathbf{x}^0 = \left(x_1^{\,0}, x_2^{\,0}, \cdots, x_n^{\,0}\right)$ and $\mathbf{y}^0 = \left(y_1^{\,0}, y_2^{\,0}, \cdots, y_n^{\,0}\right)$. If $x_i^0 \neq y_i^0$, we define two fuzzy sets, $\left(A_i^1, \mu_{A_i^1}\right)$ and $\left(A_i^2, \mu_{A_i^2}\right)$, in the l th subspace of U, with

$$\mu_{A_i^1}(x_i) = \exp\left[-\frac{\left(x_i - x_i^{\,0}\right)^2}{2}\right] \tag{a6}$$

$$\mu_{A_i^2}(x_i) = \exp\left[-\frac{\left(x_i - y_i^{\,0}\right)^2}{2}\right] \tag{a7}$$

If $x_i^0 = y_i^0$, then $A_i^1 = A_i^2$ and $\mu_{A_i^2} = \mu_{A_i^2}$. That is, only one fuzzy set is defined in the l th subspace of U. We define two fuzzy sets, (B^1, μ_{B^1}) and (B^2, μ_{B^2}), in the output universe of discourse R, with

$$\mu_{B^j}(z) = \exp\left[-\frac{(z - \bar{z}^j)^2}{2}\right] \tag{a8}$$

where $j = 1, 2$, and $\bar{z}^j$ will be specified later. We choose two fuzzy rules for the fuzzy rule base (that is, $M = 2$). Now we have specified all the design parameters except $\bar{z}^j$ $(j = 1, 2)$. That is, we have already obtained a function f which is in the form of (3.35) with $M = 2$. With this f, we have

$$f(\mathbf{x}^0) = \frac{\bar{z}^1 + \bar{z}^2 \prod_{i=1}^{n} \exp\left[-(x_i^0 - y_i^0)^2/2\right]}{1 + \prod_{i=1}^{n} \exp\left[-(x_i^0 - y_i^0)^2/2\right]} = \alpha \bar{z}^1 + (1 - \alpha)\bar{z}^2 \tag{a9}$$

$$f(\mathbf{y}^0) = \frac{\bar{z}^2 + \bar{z}^1 \prod_{i=1}^{n} \exp\left[-(x_i^0 - y_i^0)^2/2\right]}{1 + \prod_{i=1}^{n} \exp\left[-(x_i^0 - y_i^0)^2/2\right]} = \alpha \bar{z}^2 + (1 - \alpha)\bar{z}^1 \tag{a10}$$

where

$$\alpha = \frac{1}{1 + \prod_{i=1}^{n} \exp\left[-(x_i^0 - y_i^0)^2/2\right]} \tag{a11}$$

Since $\mathbf{x}^0 \neq \mathbf{y}^0$, there must be some l such that $x_i^0 \neq y_i^0$; hence, we have $\prod_{i=1}^{n} exp\left[-(x_i^0 - y_i^0)^2/2\right] \neq 1$, or, $\alpha \neq 1 - \alpha$. If we choose $\bar{z}^1 = 0$ and $\bar{z}^2 = 1$, then $f(\mathbf{x}^0) = 1 - \alpha \neq \alpha = f(\mathbf{y}^0)$.   Q.E.D.

Lemma A.3: (Y, d_∞) vanishes at no point of U.

Proof: By observing (3.35), we simply choose all $\bar{y}^l > 0$ $(l = 1, 2, \cdots, M)$, that is, any $f \in Y$ with $\bar{y}^j > 0$ serves as the required f.   Q.E.D.

Proof of the Universal Approximation Theorem : From (3.35), it is obvious that Y is a set of real continuous functions on U. The Universal Approximation Theorem is therefore a direct consequence of the Stone-Weierstrass Theorem and Lemmas A.1-A.3.   Q.E.D.

Appendix B. Proof of Theorem 2

(i) **a**. Equation (3.58)

Let $V_\theta = \frac{1}{2}\Theta^T\Theta$. If Equation (3.55) is true, we have either $|\Theta| < M_\theta$ or $\dot{V}_\theta = \gamma\mathbf{e}^T\mathbf{p}_n\Theta^T\Xi(\mathbf{x}) \le 0$ when $|\Theta| = M_\theta$; i.e., we always have $|\Theta| \le M_\theta$. If Equation (3.56) is true, we have $|\Theta| = M_\theta$ and $\dot{V}_\theta = \gamma\mathbf{e}^T\mathbf{p}_n\Theta^T\Xi(\mathbf{x}) - \gamma\mathbf{e}^T\mathbf{p}_n\frac{|\Theta|^2\Theta^T\Xi(\mathbf{x})}{|\Theta|^2} = 0$; i.e., $|\Theta| \le M_\theta$. Therefore, we always have $|\Theta| \le M_\theta$, for all $t \ge 0$.

b. Equation (3.59)

In section III.2.2.3 we proved that $V_e \le \overline{V}$; therefore, $\frac{1}{2}\lambda_{min}|\mathbf{e}|^2 \le \frac{1}{2}\mathbf{e}^T\mathbf{Pe} \le \overline{V}$, i.e., $|\mathbf{e}| \le \left(\frac{2\overline{V}}{\lambda_{min}}\right)^{1/2}$. Since $\mathbf{e} = \mathbf{x}_d - \mathbf{x}$, we have $|\mathbf{x}(t)| \le |\mathbf{x}_d| + |\mathbf{e}| \le |\mathbf{x}_d| + \left(\frac{2\overline{V}}{\lambda_{min}}\right)^{1/2}$, which is (3.59)

c. Equation (3.60)

Since $u_c(\mathbf{x}|\Theta)$ is a weighted average of the elements of Θ, we have $u_c(\mathbf{x}|\Theta) \le \Theta \le M_\theta$. Therefore, from (3.39) and (3.46) we have (3.60)

(ii) From (3.54), (3.55), and (3.56), we have

$$\dot{V} = -\frac{1}{2}\mathbf{e}^T\mathbf{Qe} - \mathbf{e}^T\mathbf{Pb}_c u_s - \mathbf{e}^T\mathbf{Pb}_c w + I_1\mathbf{e}^T\mathbf{p}_n b\frac{\Phi^T\Theta\Theta^T\Xi(\mathbf{x})}{|\Theta|^2}, \qquad (b1)$$

where $I_1 = 0$ if (3.55) is true, and $I_1 = 1$ if (3.56) is true. Now we show that the last term of (b1) is nonpositive. If $I_1 = 0$, the conclusion is trivial. Let $I_1 = 1$, which means that $|\Theta| = M_\theta$ and $\mathbf{e}^T\mathbf{p}_n\Theta^T\Xi(\mathbf{x}) > 0$; we have $\Phi^T\Theta = (\Theta^* - \Theta)^T\Theta = \frac{1}{2}\left[|\Theta^*|^2 - |\Theta|^2 - |\Theta - \Theta^*|^2\right] \le 0$, since $|\Theta| = M_\theta \ge |\Theta^*|$. Therefore, the last term of (b1) is nonpositive, and we have

$$\dot{V} \le -\frac{1}{2}\mathbf{e}^T\mathbf{Qe} - \mathbf{e}^T\mathbf{Pb}_c u_s - \mathbf{e}^T\mathbf{Pb}_c w. \qquad (b2)$$

From (3.46) we have $\mathbf{e}^T\mathbf{Pb}_c u_s \ge 0$; therefore, (b2) can be further simplified to

$$\dot{V} \le -\frac{1}{2}\mathbf{e}^T\mathbf{Q}\mathbf{e} - \mathbf{e}^T\mathbf{Pb}_c w$$

$$\le -\frac{\lambda_{Q\min}-1}{2}|\mathbf{e}|^2 - \frac{1}{2}\left[|\mathbf{e}|^2 + 2\mathbf{e}^T\mathbf{Pb}_c w + |\mathbf{Pb}_c w|^2\right] + \frac{1}{2}|\mathbf{Pb}_c w|^2$$

$$\le -\frac{\lambda_{Q\min}-1}{2}|\mathbf{e}|^2 + \frac{1}{2}|\mathbf{Pb}_c w|^2, \qquad\qquad (b3)$$

where $\lambda_{Q\min}$ is the minimum eigenvalue of Q. Integrating both sides of (b3) and assuming that $\lambda_{Q\min} > 1$ (since Q is determined by the designer, we can choose such a Q), we have

$$\int_0^t |\mathbf{e}(\tau)|^2 d\tau \le \frac{2}{\lambda_{Q\min}-1}\left[|V(0)| + |V(t)|\right] + \frac{1}{\lambda_{Q\min}-1}|\mathbf{Pb}_c|^2\int_0^t |w(\tau)|^2 d\tau \qquad (b4)$$

Define $a = \frac{2}{\lambda_{Q\min}-1}\left[|V(0)| + \sup_{t\ge0}|V(t)|\right]$ and $c = \frac{1}{\lambda_{Q\min}-1}|\mathbf{Pb}_c|^2$. Equation (b4) becomes (3.61) (note that $\sup_{t\ge0}|V(t)|$ is finite because $\mathbf{e}$ and Φ are all bounded).

(iii) If $w \in L_2$, then from (3.61) we have $\mathbf{e} \in L_2$. Because we have proved that all the variables on the right-hand side of (3.50) are bounded, we have $\dot{\mathbf{e}} \in L_\infty$. Using Barbalat's lemma (if $\mathbf{e} \in L_2 \cap L_\infty$ and $\dot{\mathbf{e}} \in L_\infty$, then $\lim_{t\to\infty}|\mathbf{e}(t)| = 0$.   Q.E.D.

Appendix C. Vehicle model parameters

variable	*description*		*value*	
I_x	moment of inertia about x-axis		479.6	[kg-m^2]
I_y	moment of inertia about y-axis		2549.3	[kg-m^2]
I_z	moment of inertia about z-axis		2782.7	[kg-m^2]
J_{eng}	engine inertia		0.2630	[kg-m^2]
$J_{gear}(i)$	i^{th} gear inertia	(1)	0.07582	[kg-m^2]
		(2)	0.08202	
		(3)	0.11388	
		(4)	0.13150	
J_w	wheel inertia		1.2825	[kg-m^2]
m	vehicle mass		1573	[kg]
h_0	vertical distance to c.g		0.487	[m]
h_2	vertical distance from c.g. to roll center	0.30		[m]
h_4	vertical distance from c.g. to pitch center		0.25	[m]
h_5	long. distance from c.g. to pitch center		0.10	[m]
l_1	distance from c.g. to front axle		1.034	[m]
l_2	distance from c.g. to rear axle		1.491	[m]
S_b	track of vehicle		1.450	[m]
r_w	wheel radius		.3044	[m]
C_{sf}	cornering stiffness of front tire		66366	[N]
C_{sr}	cornering stiffness of rear tire		52812	[N]
F_{roll}	total tire rolling resistance		274.7	[N]
MAX	maximum manifold intake airflow		684.109	
T_{man}	manifold temperature		310.93	[C$^\circ$]
V_{man}	manifold volume		0.00447	[L]
c_x	wind drag coefficient x-dir		.45	
c_y	wind drag coefficient y-dir		2.1	
$r_{gear}(i)$	i^{th} gear ratio	(1)	0.4167	
		(2)	0.6817	
		(3)	1.0000	
		(4)	1.4993	

Appendix D. Simplified Vehicle Model (SVM)

In this appendix, the simplified vehicle model used for control design is derived from the full simulation model. All assumptions are stated. To reiterate, the vehicle model is expressed by the following 12 state equations.

$$m[\dot{V}_x - V_y\dot{\psi} + h_4\ddot{\theta} + h_2\dot{\phi}\dot{\psi} + h_2\phi\ddot{\psi}] = \sum_{i=1}^{4} F_{A_i} - C_x V_x^2 - F_{roll} \tag{d1}$$

$$m[\dot{V}_y + V_x\dot{\psi} - h_2\ddot{\phi} + h_4\dot{\theta}\dot{\psi} + h_4\theta\ddot{\psi}] = \sum_{i=1}^{4} F_{B_i} - C_y V_y^2 \tag{d2}$$

$$m[\dot{V}_z + V_x\dot{\chi}\beta - h_5\ddot{\theta}] = \sum_{i=1}^{4} F_{P_i} - mg \tag{d3}$$

$$I_x[\ddot{\phi} - \theta\ddot{\psi} - \dot{\theta}\dot{\psi}] - (I_y - I_z)\dot{\theta}\dot{\psi} = M_x - \theta M_z \tag{d4}$$

$$I_y[\ddot{\theta} + \phi\ddot{\psi} + \dot{\phi}\dot{\psi}] - (I_z - I_x)\dot{\phi}\dot{\psi} = M_y + \phi M_z \tag{d5}$$

$$I_z[\ddot{\psi} + \theta\ddot{\phi} - \ddot{\theta}\phi] - (I_x - I_y)\dot{\theta}\dot{\phi} = M_z + \theta M_x - \phi M_y \tag{d6}$$

$$J_{wi}\dot{\omega}_{wi} = \frac{1}{2}T_{shaft} - \frac{3}{10}T_{brake} - r_{wi}F_{xi} \qquad i = 1,2$$

$$J_{wi}\dot{\omega}_{wi} = -\frac{1}{5}T_{brake} - r_{wi}F_{xi} \qquad i = 3,4 \tag{d7}$$

$$\dot{\omega}_{eng} = \frac{1}{J_{eng}}[T_{net} - T_{pump}] \tag{d8}$$

$$\dot{m}_{air} = \dot{m}_{air\,in} - \dot{m}_{air\,out} \tag{d9}$$

$$\dot{\alpha} = \frac{1}{\tau_{throt}}[\alpha_{com} - \alpha] \tag{d10}$$

$$\dot{T}_{brake} = \frac{1}{\tau_{brake}}[T_{brk\,com} - T_{brake}] \tag{d11}$$

$$\dot{\delta}_f = \frac{1}{\tau_{steer}}[\delta_{com} - \delta_f] \tag{d12}$$

By neglecting actuator and manifold dynamics and the roll (θ), pitch (ϕ), and vertical (z) motions, the model can be reduced to:

$$m[\dot{V}_x - V_y \dot{\psi}] = \sum_{i=1}^{4} F_{A_i} - C_x V_x^2 - F_{roll} \tag{d13}$$

$$m[\dot{V}_y + V_x \dot{\psi}] = \sum_{i=1}^{4} F_{B_i} - C_y V_y^2 \tag{d14}$$

$$I_z \ddot{\psi} = M_z \tag{d15}$$

$$J_{wi} \dot{\omega}_{wi} = \frac{1}{2} T_{shaft} - \frac{3}{10} T_{brake} - r_{wi} F_{xi} \qquad i = 1,2$$

$$J_{wi} \dot{\omega}_{wi} = -\frac{1}{5} T_{brake} - r_{wi} F_{xi} \qquad i = 3,4 \tag{d16}$$

$$\dot{\omega}_{eng} = \frac{1}{J_{eng}} [T_{net} - T_{pump}] \tag{d17}$$

The x-moment about the unsprung mass, M_x, can be expressed as:

$$M_z = l_1 (F_{B_1} + F_{B_2}) - l_2 (F_{B_3} + F_{B_4}) - \frac{S_{b1}}{2}(F_{A_1} - F_{A_2}) - \frac{S_{b2}}{2}(F_{A_3} - F_{A_4}) \tag{d18}$$

Under the bicycle model assumption (*i.e.* the dynamics of the left and right side of the vehicle are identical), the moment expression becomes:

$$M_z = 2l_1 (F_{B_f}) - 2l_2 (F_{B_r}) \tag{d19}$$

The external forces are:

$$\sum_{i=1}^{4} F_{A_i} = 2(F_{x_f} - \delta_f F_{y_f}) + 2F_{x_r} \qquad (\delta_r = 0) \tag{d20}$$

$$\sum_{i=1}^{4} F_{B_i} = 2(F_{y_f} - \delta_f F_{x_f}) + 2F_{y_r} \tag{d21}$$

where,

$$F_{x_f} = F_{x_1} = F_{x_2} , \text{ etc.}$$

Noting that the following is true:

$$F_{y_f} - \delta_f F_{x_f} = C_{s_f}(\delta_f - \zeta_f) - \delta_f F_{x_f}$$
$$\Rightarrow \qquad = \delta_f(C_{s_f} - F_{x_f}) - C_{s_f}\zeta_f$$
$$\Rightarrow \qquad \approx C_{s_f}\delta_f - C_{s_f}\zeta_f = F_{y_f} \qquad (C_{s_f} \gg F_{x_f})$$

the lateral forces can be rewritten as:

$$\sum_{i=1}^{4} F_{B_i} \approx 2F_{y_f} + 2F_{y_r} \qquad\qquad (d22)$$

Further, by assuming that $\dot{\omega}_{w_f} = \dot{\omega}_{w_r}$, The simplified state equations (d13-17) is reduced to:

$$\dot{V}_x = -\frac{1}{m}[C_x V_x^2 + F_{roll} - mV_y\dot{\psi} - 2(F_{x_f} + F_{x_r}) - 2\delta_f F_{y_f}] \qquad (d23)$$

$$\dot{V}_y = -\frac{1}{m}[C_y V_y^2 - mV_x\dot{\psi} - 2(F_{y_f} + F_{y_r})] \qquad (d24)$$

$$\dot{\psi} = \frac{2}{I_z}[l_1 F_{y_f} - l_2 F_{y_r}] \qquad (d25)$$

$$\dot{\omega}_w = \frac{1}{4J_w}[T_{shaft} - T_{brake} - 2r_w(F_{x_f} + F_{x_r})] \qquad (d26)$$

$$\dot{\omega}_{eng} = \frac{1}{J_{eng}}[T_{net} - T_{pump}] \qquad (d27)$$

The engine and brake torques, T_{net} and T_{brake}, can be related to the traction forces by assuming that the torque converter is locked. In other words, we assume:

i) $\qquad \omega_{eng} \approx \dfrac{\omega_w}{r^*}$

ii) $\qquad T_{pump} \approx r^* T_{shaft}$

where $r^* = r_{drive}r_{gear}$ is the effective gear ratio.

Under this assumption, the engine and wheel accelerations (d26-27) can be combined to yield:

(a) $\dot{\omega}_{eng} = \dfrac{1}{J_{eng}}[T_{net} - r^* T_{shaft}]$

$\Rightarrow \qquad T_{shaft} = \dfrac{1}{r^*}[T_{net} - J_{eng}\dot{\omega}_{eng}]$

$\Rightarrow \qquad T_{shaft} = \dfrac{1}{r^*}[T_{net} - J_{eng}\dfrac{\dot{\omega}_w}{r^*}]$

(b) $\dot{\omega}_w = \dfrac{1}{4J_w}[T_{shaft} - T_{brake} - r_w F_{x_{tot}}]$

$\Rightarrow \qquad \dot{\omega}_w = \dfrac{1}{4J_w}[\dfrac{1}{r^*}(T_{net} - J_{eng}\dfrac{\dot{\omega}_w}{r^*}) - T_{brake} - r_w F_{x_{tot}}]$

$\Rightarrow \qquad \dot{\omega}_w[J_{eng} + 4J_w r^{*2}] = [r^* T_{net} - r^{*2} T_{brake} - r_w r^{*2} F_{x_{tot}}]$

Solving for $F_{x_{tot}}$ and substituting this into eq d23 yields:

$$F_{x_{tot}} = \dfrac{1}{r_w r^{*2}}[r^* T_{net} - r^{*2} T_{brake} - \dot{\omega}_w(J_{eng} + 4J_w r^{*2})]$$

$\Rightarrow \qquad \dot{V}_x[1 + \dfrac{1}{mr_w^2 r^{*2}}(J_{eng} + 4J_w r^{*2})] = -\dfrac{1}{m}[C_x V_x^2 + F_{roll} - mV_y\dot{\psi} -$

$$\dfrac{1}{r_w r^*}(T_{net} - r^* T_{brake}) + \delta_f F_{y_f}]$$

Define:

$J^* = mr_w^2 r^{*2} + J_{eng} + 4J_w r^{*2}$

$T_{tot} = T_{net} - r^* T_{brake}$

The final form of the state equations of the simplified vehicle model is now:

$$\dot{V}_x = -\dfrac{(r_w r^*)^2}{J^*}[C_x V_x^2 + F_{roll} - mV_y\dot{\psi}] + \dfrac{(r_w r^*)^2}{J^*}[\dfrac{1}{r_w r^*}T_{tot} + \delta_f F_{y_f}] \qquad \text{(d28)}$$

$$\dot{V}_y = -\dfrac{1}{m}[C_y V_y^2 - mV_x\dot{\psi} - 2(F_{y_f} + F_{y_r})] \qquad \text{(d29)}$$

$$\ddot{\psi} = \dfrac{2}{I_z}[l_1 F_{y_f} - l_2 F_{y_r}] \qquad \text{(d30)}$$

Appendix E. Tire model (Bakker-Pacjeka)
(Fitted on Yokohoma P205/60R1487H steel-belted radials)

$$F_x = D_x \sin(C_x \tan^{-1}(B_x \phi_x)) + S_{vx} \tag{e1}$$

$$F_y = D_y \sin(C_y \tan^{-1}(B_y \phi_y)) + S_{vy} \tag{e2}$$

$$\phi_x = (1 - E_x)(i_s + S_{hx}) + \frac{E_x}{B_x} \tan^{-1}(B_x(i_s + S_{hx})) \tag{e3}$$

$$\phi_y = (1 - E_y)(v + S_{hy}) + \frac{E_y}{B_y} \tan^{-1}(B_y(v + S_{hy})) \tag{e4}$$

traction ($i_s > 0$)	_braking ($i_s \leq 0$)_

$$B_x = 22 + \frac{F_z - 1940}{645} \qquad\qquad B_x = 22 + \frac{F_z - 1940}{430}$$

$$C_x = 1.35 - \frac{F_z - 1940}{16125} \qquad\qquad C_x = 1.35 - \frac{F_z - 1940}{16125}$$

$$D_x = 1750 + \frac{F_z - 1940}{.956} \qquad\qquad D_x = 1750 + \frac{F_z - 1940}{.956}$$

$$E_x = -3.6 \qquad\qquad\qquad\qquad E_x = 0.1$$

$$S_{hx} = 0 \qquad\qquad\qquad\qquad S_{hx} = 0$$

$$S_{vx} = 0 \qquad\qquad\qquad\qquad S_{vx} = 0$$

$$B_y = 0.22 + \frac{5200 - F_z}{40000}$$

$$C_y = 1.26 + \frac{F_z - 5200}{32750}$$

$$D_y = -0.00003 F_z^2 + 1.0096 F_z - 22.73$$

$$E_x = -1.6$$

$$S_{hy} = 0$$

$$S_{vy} = 0$$

References

[1] H. Peng, and M. Tomizuka, "Vehicle lateral control for highway automation", Proceedings of the 1990 American Control Conference, San Diego, 1990.

[2] H. Leiber and A. Czinczel, "Four years of Experience with 4-wheel anti-skid brake(ABS) , SAE 830481, 1983.

[3] H. Leiber et al. ,"Anti-Skid system (ABS) for passenger Cars", Bosch Technical and Scientific Report, 1982.

[4] S. Yoneda, Y. Naitoh, and H. Kigoshi, "Rear brake lock-up control system of Mitsubishi Starion", SAE paper 830482, 1983.

[5] H. Tan, "Adaptive and robust controls with Application to Vehicle Traction Control", Ph. D. Dissertation, University of California, Berkeley, 1988.

[6] H. Tan, and M. Tomizuka, "A Discrete- Time Robust Vehicle Traction Controller Design ", Proceedings of the 1989 American Control Conference, Pittsburgh, 1989.

[7] H. Tan, and M. Tomizuka, "An adaptive Sliding Mode Vehicle Traction Controller Design", Proceedings of the 1990 American Control Conference, San Diego, 1990

[8] R. Fling and R. Fenton, "A describing-function approach to anti-skid design", IEEE Trans. on Vehicular Technology Vol. 30, Aug. 1981.

[9] T. Tabo, N. Ohka, H. Kuraoka, and M. Ohba, " Automotive anti-skid system using modern control theory", Proceedings of the 1985 IECON, 1985.

[10] R. Gunter and H. Ouwerkerk, " Adaptive brake control system", Proceedings on Instit. Mech. Eng., Vol.186, 1972.

[11] J. Layne, K. Passino, and S. Yurkovich, " Fuzzy Learning Control for Antiskid Braking Systems ", IEEE Trans. on Control System Tech., Vol. 1, No. 2, June 1993.

[12] P. Kachroo, and M. Tomizuka, " Vehicle traction control and its Application", Publication of PATH project, ITS, UC Berkeley, UCB-ITS-PRR-94-08, March 1994.

[13] P. Kachroo, " Nonlinear Control Strategies and Vehicle Traction Control", Ph.D. dissertation, UC Berkeley, November 1993.

[14] K. Hedrick, et al.," Longitudinal vehicle controller design for IVHS Systems", Proceedings of the 1990 American Control Conference, San Diego, 1990.

[15] S. Taheri, E. Law, " Investigation of Integrated Slip Control Braking and Closed Loop Four Wheel Steering Systems for Automobiles during Combined Hard Braking and Severe Steering ", Proceedings of the 1990 American Control Conference, San Diego, 1990.

[16] C. Lee, " Fuzzy Logic in Control Systems: Fuzzy Logic Controller-Part I ", IEEE Trans. on Syst., Man, Cybern., Vol.20, Mar./Apr. 1990.

[17] C. Lee, " Fuzzy Logic in Control Systems: Fuzzy Logic Controller-Part II ", IEEE Trans. on Syst., Man, Cybern., Vol.20, Mar./Apr. 1990.

[18] J.-J. E. Slotine, W. Li, " Applied Nonlinear Control ", Prentice-Hall Inc.,1990.

[19] Li-Xin Wang, "Stable Adaptive Fuzzy Control of Nonlinear Systems", IEEE Trans. on Fuzzy Systems, Vol.1, No.2, May 1993.

[20] D. H. McMahon, J. K. Hedrick, S. E. Shladover, " Vehicle Modelling and Control for Automated Highway System," Proceedings of the 1991 American Control Conference, Boston, 1991.

[21] H. Peng, " Vehicle Lateral Control for Highway Automation," Ph.D. dissertation, UC Berkeley, 1992.

[22] H. Pham, Master Thesis, UC Berkeley, 1992.

[23] M. Tomizuka and J.K.Hedrick, " Automated Vehicle Control for IVHS Systems", Proceedings of the 1991 World Congress of International Federation Automatic Control Conference, Sydney, Australia, 1993.

[24] J. Y. Wong, " Theory of Ground Vehicles", Wiley, New York, 1978.

[25] W. Pedrycz, " Fuzzy Control and Fuzzy Systems", John Wiley & Sons, New York, 1989.

[26] Li-Xin Wang and J. M. Mendel, "Fuzzy Basis Functions, Universal Approximation, and orthogonal Least squares learning", IEEE Trans. on Neural Networks, Vol. 3, 1992.

[27] T. Poggio and F. Girosi, "Networks for approximation and learning", Proceedings of IEEE, Vol. 78, 1990.

[28] W. Rudin, "Principles of Mathematical Analysis, McGraw-Hill, New York, 1976.

[29] K. S. Narendra and K. Parthasarathy, "Identification and Control of Dynamic Systems using Neural Networks", IEEE Trans. on Neural Networks, Vol. 1, 1990.

[30] K. S. Narendra and A. M. Annaswamy, "Stable Adaptive Systems", Englewood Cliffs, NJ: Prentice-Hall, 1989.

[31] K. S. Chang, et al., "Experimentation with a Vehicle Platoon Control System", Proceedings of the 1991 Vehicle Navigation and Information System Conference, Dearborn, 1991